

Synthesis, Characterization, and Reactivity of New Alkynyl Complexes of Rhodium and Iridium: Preparation of Neutral (M–M': M = Rh, Ir; M' = Pt, Pd) Hetero-Alkynyl-Bridged Dinuclear Complexes

Irene Ara,[†] Jesús R. Berenguer,[‡] Eduardo Eguizábal,[‡] Juan Forniés,^{*,†} Elena Lalinde,^{*,‡} Antonio Martín,[†] and Francisco Martínez[†]

Departamento de Química Inorgánica, Instituto de Ciencia de Materiales de Aragón, Universidad de Zaragoza-Consejo Superior de Investigaciones Científicas, 50009 Zaragoza, Spain, and Departamento de Química, Universidad de La Rioja, 26001 Logroño, Spain

Received May 4, 1998

The alkynylation of [Cp*MX₂(PEt₃)] (Cp* = η⁵-C₅Me₅; X = Cl, M = Rh; X = I, M = Ir) with an excess of LiC≡CR (R = Ph (**a**), ^tBu (**b**), SiMe₃ (**c**)) in thf leads to novel bis(alkynyl) [Cp*M(C≡CR)₂(PEt₃)] (M = Rh, **3a–c**; M = Ir, **4a,c**) or mono(alkynyl) [Cp*M(C≡CR)X(PEt₃)] (M = Rh, X = Cl, **1a–c**; M = Ir, X = I, **2c'**) complexes depending on the reaction time. Complex **4a** and the related (phenylethynyl)iridium derivatives [Cp*Ir(C≡CPh)X(PEt₃)] (X = Cl, **2a**; X = I, **2a'**) can be prepared by reacting [Cp*IrX₂(PEt₃)] with [AgC≡CPh]_n. Complexes **1–4** undergo facile reaction with [*cis*-M'(C₆F₅)₂(thf)₂] (M' = Pt, Pd; thf = tetrahydrofuran), affording homobridged bis(μ-alkynyl) [(PEt₃)Cp*M(μ-C≡CR)₂M'(C₆F₅)₂] (M = Rh, M' = Pt (**5a,c**), Pd (**6a,c**); M = Ir, M' = Pt (**7a,c**), Pd (**8a,c**)) or heterobridged μ-alkynyl-μ-halide [(PEt₃)Cp*M(μ-C≡CR)(μ-X)M'(C₆F₅)₂] (M = Rh, X = Cl, M' = Pt (**9a–c**), Pd (**10a,b**); M = Ir, X = Cl, I, M' = Pt (**11a,a',c'**), Pd (**12a,a',c'**)) heterodinuclear compounds. Complexes **5a,c** and **7a,c** can, alternatively, be obtained through a neutralization reaction between the dianionic complexes Q₂[*cis*-Pt(C₆F₅)₂(C≡CR)₂] (R = Ph, Q = PMePh₃; R = SiMe₃, Q = NBu₄) and solvento species [Cp*M(PEt₃)(acetone)₂](ClO₄)₂ (M = Rh, Ir) (prepared in situ). The molecular structures of the heterobridged Rh–Pt (**9b**) and Ir–Pd (**12a**) and homobridged Rh–Pt (**5c**), Ir–Pt (**7a,c**), and Ir–Pd (**8a**) complexes have been determined by X-ray analyses. In the iridium mixed complexes **7a,c**, **8a**, and **12a** the alkynyl ligands are σ-bonded to iridium and π-bonded to Pt (**7a,c**) or Pd (**8a**, **12a**) centers. In contrast, the crystal structure of **5c** shows a dinuclear zwitterionic complex formed by two different alkynyl organometallic termini, [Cp*Rh⁺(C≡CSiMe₃)(PEt₃)] and [*cis*-Pt⁻(C₆F₅)₂(C≡CSiMe₃)], held together through η²-bonding of the alkynyl groups.

Introduction

The chemistry of transition-metal alkynyl and related complexes has been studied extensively and continues to be the focus of considerable attention.¹ The interest in such complexes is due to different factors, including (i) the ability of alkynide ligands to adopt various coordination modes,^{1a–e,2} (ii) their relationship with vinylidene complexes,³ (iii) the possibility of a variety

of interesting ligand-based coupling and cycloaddition reactions,⁴ and (iv) their involvement in catalysis and in the preparation of new materials.^{2a,5} In this area, particular attention has been paid to homo- and heterodinuclear complexes stabilized by a double-alkynyl bridging system, M(μ-C≡CR)₂M',⁶ because of their relevance in C–C coupling alkynide processes,⁷ as well as C–C bond cleavage on butadiynes⁸ induced by metal centers. Considerable experimental work^{6–8} and recent theoretical calculations by Jemmis *et al.*⁹ on homodinuclear Ti and Zr complexes seem to indicate the existence of a delicate thermodynamic balance between coupled and uncoupled structures. The different factors (metal and substituents) that affect these processes could be related to the factors that govern the preferential geometry of the alkynyl ligands on these double-alkynide-bridged compounds L_nM(μ-C≡CR)₂M'L'_n.⁶ The preferential formation of symmetrical (μ-σ-M₂C₂ cores, **Ia,b**),¹⁰ unsymmetrical (σ/π planar (**IIa**) or hinged (**IIb**) (M₂C₄ cores),^{7b,8b–e,h,11} chelating (tweezer-like (**IIIa**) or V-shaped (**IIIb**)),^{2c,6,8g,12} or intermediate arrangements

[†] Universidad de Zaragoza-Consejo Superior de Investigaciones Científicas.

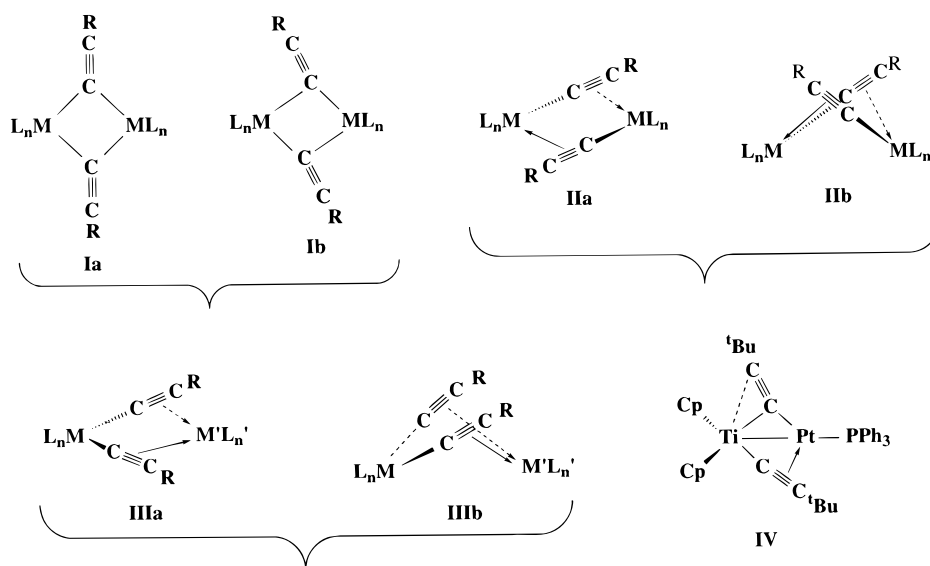
[‡] Universidad de La Rioja.

(1) (a) Nast, R. *Coord. Chem. Rev.* **1982**, *47*, 89. (b) Carty, A. J. *Pure Appl. Chem.* **1982**, *54*, 113. (c) Sappa, E.; Tiripicchio, A.; Braunstein, P. *Coord. Chem. Rev.* **1985**, *65*, 219. (d) Akita, M.; Moro-Oka, Y. *Bull. Chem. Soc. Jpn.* **1995**, *68*, 420. (e) Forniés, J.; Lalinde, E. *J. Chem. Soc., Dalton Trans.* **1996**, 2587 and references therein. (f) Manna, J.; John, K. D.; Hopkins, M. D. *Adv. Organomet. Chem.* **1995**, *38*, 79.

(2) (a) Beck, V.; Niemer, B.; Wieser, M. *Angew. Chem., Int. Ed. Engl.* **1993**, *32*, 923. (b) Lotz, S.; van Rooyen, P. H.; Meyer, R. *Adv. Organomet. Chem.* **1995**, *37*, 219. (c) Lang, H.; Köhler, K.; Blau, S. *Coord. Chem. Rev.* **1995**, *143*, 113.

(3) (a) Bruce, M. I. *Chem. Rev.* **1991**, *91*, 197. (b) Davies, S. G.; McNally, J. P.; Smallridge, A. J. *Adv. Organomet. Chem.* **1990**, *30*, 1. (c) Werner, H. J. *Organomet. Chem.* **1994**, *475*, 45. (d) Werner, H. J. *Chem. Soc., Chem. Commun.* **1997**, 903.

Chart 1



(IV)^{11d} (Chart 1) is still a matter of speculation, although it is clear that the final structures are governed by electronic and steric factors both on the metal centers (ML_n) and on the alkynyl ligands (R substituents).

Several years ago we observed that the tetrahydrofuran molecules on [cis-Pt(C₆F₅)₂(thf)₂] are easily displaced by diphenylacetylene^{13a} or by the alkyne fragments of neutral cis-bis(alkynyl)platinum building blocks. In the latter, dinuclear {cis,cis-[L₂Pt(C≡CR)₂]Pt(C₆F₅)₂} complexes containing a bent chelating type (V-shaped, type IIIb; Chart 1) double-alkynyl bridging system were

obtained.^{13b} However, treatment of [cis-Pt(C₆F₅)₂(thf)₂] with anionic Q₂[cis-Pt(C₆F₅)₂(C≡CR)₂] leads to σ/π-alkynide-bridged complexes Q₂[Pt(μ-σ:η²-C≡CR)(C₆F₅)₂]₂ (type II; Chart 1) formed via a formal migration of one

(4) (a) Wrackmeyer, B.; Horchler, K.; Boese, R. *Angew. Chem., Int. Ed. Engl.* **1989**, *28*, 1500. (b) Cherkas, A. A.; Randall, L. H.; Taylor, N. J.; Mott, G. N.; Yule, J. E.; Guinamant, J. L.; Carty, A. J. *Organometallics* **1990**, *9*, 1677 and references therein. (c) Wong, A.; Pawlick, R. V.; Thomas, C. G.; Lean, D. R.; Liu, L.-K. *Organometallics* **1991**, *10*, 530. (d) St. Clair, M.; Schaefer, W. P.; Bercaw, J. E. *Organometallics* **1991**, *10*, 526. (e) Selegue, J. P.; Young, B. A.; Logan, S. L. *Organometallics* **1991**, *10*, 1972. (f) García Alonso, F. J.; Riera, V.; Ruiz, M. A.; Tiripicchio, A.; Tiripicchio Camellini, M. *Organometallics* **1992**, *11*, 370. (g) Lemke, F. R.; Bullock, R. M. *Organometallics* **1992**, *11*, 4261. (h) Field, L. D.; George, A. V.; Purches, G. R.; Slip, I. H. M. *Organometallics* **1992**, *11*, 3019. (i) Terry, M. R.; Kelley, C.; Lugan, N.; Geoffroy, G. L.; Haggerty, B. S.; Rheingold, A. L. *Organometallics* **1993**, *12*, 3607 and references therein. (j) Connelly, N. G.; Gamasa, M. P.; Gimeno, J.; Lapinte, C.; Lastra, E.; Maher, J. P.; Le Narvor, N.; Rieger, A. L.; Rieger, P. H. *J. Chem. Soc., Dalton Trans.* **1993**, 2575. (k) Matsuzaka, H.; Hirayama, Y.; Nishio, M.; Mizobe, Y.; Hidai, M. *Organometallics* **1993**, *12*, 36. (l) Shin, K.-Y.; Schrock, R. R.; Kempe, R. *J. Am. Chem. Soc.* **1994**, *116*, 8804. (m) Weng, W.; Bartik, T.; Johnson, M. T.; Arif, A. M.; Gladysz, J. A. *Organometallics* **1995**, *14*, 889 and references therein. (n) Röttger, D.; Erker, G.; Fröhlich, R.; Grehl, M.; Silverio, S. J.; Hyla-Kryspin, I.; Gleiter, R. *J. Am. Chem. Soc.* **1995**, *117*, 10503. (o) Chi, Y.; Carty, A. J.; Blenkiron, P.; Delgado, E.; Enright, G. D.; Wang, W.; Peng, S. M.; Lee, G. H. *Organometallics* **1996**, *15*, 5269. (p) Fischer, H.; Leroux, F.; Roth, G.; Stumpf, R. *Organometallics* **1996**, *15*, 3723. (q) Bianchini, C.; Innocenti, P.; Peruzzini, M.; Romerosa, A.; Zanobini, F. *Organometallics* **1996**, *15*, 272 and references therein. (r) Yi, C. S.; Liu, N. *Organometallics* **1996**, *15*, 3968. (s) Akita, M.; Terada, M.; Moro-Oka, Y. *J. Chem. Soc., Chem. Commun.* **1997**, 265.

(5) (a) Parshall, G. W.; Ittel, S. D. *Homogeneous Catalysis*, 2nd ed.; Wiley: New York, 1992. (b) Henkelmann, J. In *Applied Homogeneous Catalysis with Organometallic Compounds*; Cornils, B., Herrmann, W. A., Eds.; VCH: New York, 1995. (c) Lang, H. *Angew. Chem., Int. Ed. Engl.* **1994**, *33*, 547. (d) Long, N. J. *Angew. Chem., Int. Ed. Engl.* **1995**, *34*, 21. (e) Laine, R. M.; Viney, C. In *Inorganic and Organometallic Polymers with Special Properties*; Laine, R. M., Ed.; Kluwer Academic: Dordrecht, The Netherlands, 1991; p 413. (f) *Inorganic Materials*; Bruce, D. W., O'Hare, D., Eds.; Wiley: Chichester, U.K., 1992. (g) Prasad, P. N.; Williams, D. J. *Nonlinear Optical Effects in Molecules and Polymers*; Wiley: New York, 1991.

(6) Ara, I.; Berenguer, J. R.; Fornies, J.; Lalinde, E. *Inorg. Chim. Acta* **1997**, *264*, 199 and references therein.

(7) (a) Sekutowski, D. G.; Stucky, G. D. *J. Am. Chem. Soc.* **1976**, *98*, 1376. (b) Cuenca, T. M.; Gómez, R.; Gómez-Sal, P.; Rodríguez, G. M.; Royo, P. *Organometallics* **1992**, *11*, 1229. (c) Evans, W. J.; Keyer, R. A.; Ziller, J. W. *Organometallics* **1990**, *9*, 2628. (d) Evans, W. J.; Keyer, R. A.; Ziller, J. W. *Organometallics* **1993**, *12*, 2618. (e) Forsyth, C. M.; Nolan, S. P.; Stern, C. L.; Marks, T. J.; Rheingold, A. L. *Organometallics* **1993**, *12*, 3618. (f) Heeres, H. J.; Nijhoff, J.; Teuben, J. H.; Rogers, R. D. *Organometallics* **1993**, *12*, 2609. (g) Duchateau, R.; van Wee, C. T.; Teuben, J. H. *Organometallics* **1996**, *15*, 2291. (h) Lee, L.; Berg, D. J.; Bushnell, G. W. *Organometallics* **1995**, *14*, 5021. (i) Takahashi, T.; Xi, Z.; Obora, Y.; Suzuki, N. *J. Am. Chem. Soc.* **1995**, *117*, 2665. (j) Hsu, P. D.; Davis, W. M.; Buckwald, S. L. *J. Am. Chem. Soc.* **1993**, *115*, 10394.

(8) (a) Pulst, S.; Arndt, P.; Heller, B.; Baumann, W.; Kempe, R.; Rosenthal, H. *Angew. Chem., Int. Ed. Engl.* **1996**, *35*, 1112 and references therein. (b) Burlakov, V. V.; Ohff, A.; Lefebvre, C.; Tillack, A.; Bauman, W.; Kempe, R.; Rosenthal, U. *Chem. Ber.* **1995**, *128*, 967. (c) Varga, V.; Mach, K.; Hiller, J.; Thewalt, U.; Sedmera, P.; Polásek, M. *Organometallics* **1995**, *14*, 1410. (d) Rosenthal, U.; Pulst, S.; Arndt, P.; Ohff, A.; Tillack, A.; Baumann, W.; Kempe, R.; Burlakov, V. V. *Organometallics* **1995**, *14*, 2961 and references therein. (e) Rosenthal, U.; Hoff, A.; Baumann, W.; Kempe, R.; Tillack, A.; Burlakov, V. V. *Organometallics* **1994**, *13*, 2903. (f) Rosenthal, U.; Ohff, A.; Tillack, A.; Baumann, W.; Görls, H. *J. Organomet. Chem.* **1994**, *488*, C4. (g) Trojanov, S. I.; Varga, V.; Mach, K. *Organometallics* **1993**, *12*, 2820. (h) Rosenthal, U.; Görls, H. *J. Organomet. Chem.* **1992**, *439*, C36.

(9) Jemmis, E. D.; Giju, K. T. *Angew. Chem., Int. Ed. Engl.* **1997**, *31*, 606.

(10) (a) Erker, G.; Albrecht, M.; Krüger, C.; Nolte, M.; Werner, S. *Organometallics* **1993**, *12*, 4979 and references therein. (b) Berenguer, J. R.; Falvello, L. R.; Fornies, J.; Lalinde, E.; Tomás, M. *Organometallics* **1993**, *12*, 6. (c) Duchateau, R.; van Wee, C. T.; Meetsma, A.; Teuben, J. H. *J. Am. Chem. Soc.* **1993**, *115*, 4931. (d) Yam, V. W.-W.; Lee, W.-K.; Cheung, K. K.; Lee, H.-K.; Leung, W.-P. *J. Chem. Soc., Chem. Commun.* **1996**, 2889. (e) Edwards, A. J.; Paver, M. A.; Raithby, P. R.; Rennie, M. A.; Russell, C. A.; Wright, D. S. *Organometallics* **1994**, *13*, 4967. (f) Olbrich, F.; Behrens, U.; Weiss, E. *J. Organomet. Chem.* **1994**, *472*, 365.

(11) (a) Erker, G.; Frömberg, W.; Benn, R.; Mynott, R.; Agermund, K.; Krüger, C. *Organometallics* **1989**, *8*, 911. (b) Berenguer, J. R.; Fornies, J.; Martínez, F.; Cubero, J.; Lalinde, E.; Moreno, M. T.; Welch, A. J. *Polyhedron* **1993**, *12*, 1797. (c) Muller, J.; Tschampell, M.; Pickardt, J. *J. Organomet. Chem.* **1988**, *355*, 513. (d) Berenguer, J. R.; Fornies, J.; Lalinde, E.; Martín, A. *Angew. Chem., Int. Ed. Engl.* **1994**, *33*, 2083.

(12) (a) Janssen, M. D.; Herres, M.; Dedieu, A.; Smeets, W. J. J.; Spek, A. L.; Grove, D. M.; Lang, H.; van Koten, G. *J. Am. Chem. Soc.* **1996**, *118*, 4817 and references therein. (b) Yamazaki, S.; Deeming, A. J. *J. Chem. Soc., Dalton Trans.* **1993**, 3051. (c) Berenguer, J. R.; Fornies, J.; Lalinde, E.; Martín, A.; Moreno, M. T. *J. Chem. Soc., Dalton Trans.* **1994**, 3343. (d) Ara, I.; Fernández, S.; Fornies, J.; Lalinde, E.; Martín, A.; Moreno, M. T. *Organometallics* **1997**, *16*, 5923. (e) Lang, H.; Köhler, K.; Zsolnai, L. *J. Chem. Soc., Chem. Commun.* **1996**, 2043.

σ -alkynyl group between the two Pt centers.^{13b} We also showed that when using $[\text{Pt}(\text{C}\equiv\text{CR})_4]^{2-}$ as metal building blocks, the monoalkynylation process only takes place with one "Pt(C₆F₅)₂" unit, whereas the reaction with 2 equiv of $[\text{cis-Pt}(\text{C}_6\text{F}_5)_2(\text{thf})_2]$ gives the trimetallic compounds $\{[(\text{C}_6\text{F}_5)_2\text{Pt}(\mu\text{-}\sigma\text{-}\eta^2\text{-C}\equiv\text{CR})(\mu\text{-}\eta^2\text{-}\sigma\text{-C}\equiv\text{CR})]\text{Pt}(\mu\text{-}\sigma\text{-}\eta^2\text{-C}\equiv\text{CR})_2\text{Pt}(\text{C}_6\text{F}_5)_2\}$ with a simultaneous presence of both chelating (V-shaped) and σ/π types of double-alkynyl bridging systems.^{13c} In view of these results, it could be speculated that the alkynylation process is possibly due to the difference in the formal charges of the metal centers involved. This would not, however, seem to be the only factor, as it was later found that not only neutral $[\text{cis-Pt}(\text{C}\equiv\text{CR})_2(\text{PPh}_3)_2]$ but also $[\text{cis-Pt}(\text{C}\equiv\text{CR})_2(\text{C}_6\text{F}_5)_2]^{2-}$ act only as chelating alkyne ligands when they react with $[\text{Pd}(\eta^3\text{-C}_3\text{H}_5)]^+$. Despite the presence of a very electrophilic cationic Pd center, no alkynylation processes were observed and highly polar species $\{[\text{Pt}(\mu\text{-}\sigma\text{-}\eta^2\text{-C}\equiv\text{CR})_2(\text{C}_6\text{F}_5)_2]\text{Pd}(\eta^3\text{-C}_3\text{H}_5)\}^{2-}$ (formally zwitterionic) were formed, clearly showing that the Pt(II) center has, in these species, a greater preference for the electron density associated with the sp α -carbon of both alkynyl groups than Pd does.^{13d,e} Lotz, van Eldik, et al. have recently observed related σ,π -bridging thiophene ligand exchange processes, suggesting a new concept dealing with preferred coordination sites for metal fragments in σ,π dimetallic complexes.^{13f}

In an attempt to gain a better understanding of the factors that determine this σ -alkynyl migration and that also have an influence on the final arrangement of the $\mu\text{-C}\equiv\text{CR}$ ligands in these systems, we were interested in studying the reactivity of $[\text{cis-Pt}(\text{C}\equiv\text{CR})_2(\text{C}_6\text{F}_5)_2]^{2-}$ (R = Ph (**a**), ^tBu (**b**), SiMe₃ (**c**)) toward the solvento Rh(III) and Ir(III) $[(\eta^5\text{-C}_5\text{Me}_5)\text{M}(\text{PET}_3)(\text{acetone})_2](\text{ClO}_4)_2$ species. Preliminary studies¹⁴ revealed that the highly acidic metal center in $[\text{Cp}^*\text{Ir}(\text{PET}_3)(\text{acetone})_2]^{2+}$ is not stabilized by complexation of the metalate $[\text{cis-Pt}(\text{C}\equiv\text{CPh})_2(\text{C}_6\text{F}_5)_2]^{2-}$ but rather that the Ir(III) center prefers the electron density associated with the sp C_α atoms of the alkynyl groups, giving the neutral $\{[(\text{PET}_3)\text{Cp}^*\text{Ir}(\mu\text{-}\sigma\text{-}\eta^2\text{-C}\equiv\text{CPh})_2]\text{Pt}(\text{C}_6\text{F}_5)_2\}$ (**7a**). This result is surprising for several reasons. First, the formation of **7a** implies an unprecedented double intramolecular alkynyl migration from Pt to Ir. Second, this process provides a neutral $[\text{Cp}^*\text{Ir}(\text{C}\equiv\text{CPh})_2(\text{PET}_3)]$ fragment which is stabilized in the final dimer. To the best of our knowledge, this complex is the first example of a bis(alkynyl)iridium(III) derivative containing a "(η^5 -ring)IrL" fragment. Although extensive studies of mononuclear alkynylrhodium or -iridium (in oxidative states I and III) complexes have been carried out,^{3c,d,15} in sharp contrast reports on related η^5 -cyclopentadienyl or substituted derivatives are exceedingly rare. The derivatives of this previously reported type are the chiral or racemic compounds $[\text{CpRh}(\text{C}\equiv\text{CR})\text{H}(\text{P}^i\text{Pr}_3)]$ (R = SiMe₃, Me, Ph),^{15l,16a} $[\text{Cp}^*\text{M}(\text{L-prolinate})(\text{C}\equiv\text{CR})]$ (R = Ph (Rh, Ir);

^tBu (Ir)),^{16b,c} and $[\text{Cp}^*\text{Ir}(\text{PMe}_3)\text{Ph}(\text{C}\equiv\text{CR})]$ (R = CO₂Et)¹⁷ and, as far as we are aware, analogous bis(alkynyl) complexes are presently unknown, although bis(alkynyl)rhodium species have been proposed as intermediates in oligomerization reactions.^{16b,18}

In this paper we report further results of the neutralization reactions between the platinate substrates $[\text{cis-Pt}(\text{C}\equiv\text{CR})_2(\text{C}_6\text{F}_5)_2]^{2-}$ and the solvento species $[\text{Cp}^*\text{M}(\text{PET}_3)(\text{acetone})_2]^{2+}$ which allow only the synthesis of the corresponding dinuclear neutral complexes **5a,c** (M = Rh) and **7a,c** (M = Ir), respectively. X-ray studies reveal that complexes **5c** and **7c** display a different bonding arrangement of the alkynyl groups which could be attributed to a change in the R substituent or to the stronger σ -alkynyl preference of Pt relative to Rh (**5c** type **IIb**, **7c** type **IIIb**; Chart 1). To clarify the reasons for this different arrangement, we have carried out the synthesis and characterization of the novel bis(alkynyl) mononuclear complexes $[\text{Cp}^*\text{M}(\text{C}\equiv\text{CR})_2(\text{PET}_3)]$ (**3**, M = Rh; **4**, M = Ir) and that of monoalkynyl $[\text{Cp}^*\text{M}(\text{C}\equiv\text{CR})\text{X}(\text{PET}_3)]$ (**1**, M = Rh, X = Cl; **2**, M = Ir, X = Cl, I) derivatives, which have been found as intermediates in their formation, and examined the reactions of **1–4** toward $[\text{cis-M}'(\text{C}_6\text{F}_5)_2(\text{thf})_2]$ (M' = Pt, Pd). The synthesis of both homobridged $\text{M}(\mu\text{-C}\equiv\text{CR})_2\text{M}'$ (**5–8**) and heterobridged $\text{M}(\mu\text{-X})(\mu\text{-C}\equiv\text{CR})\text{M}'$ (**9–12**) heteromixed Rh, Ir–Pt, Pd complexes and solid-state studies of **5c**, **7a,c**, **8a**, **9b**, and **12a** are presented.

Results

Mononuclear Derivatives. The synthesis and main reactions of the mononuclear complexes presented in this work are summarized in Scheme 1. The starting materials $[\text{Cp}^*\text{MCl}_2(\text{PET}_3)]$ (M = Rh, Ir), which have not been previously reported, have been prepared from $[\text{Cp}^*\text{MCl}_2]_2$ and PET_3 using a procedure similar to that described by Maitlis and co-workers.¹⁹

The formation of alkynylrhodium(III) derivatives was accomplished by the displacement of chloride ligands from $[\text{Cp}^*\text{RhCl}_2(\text{PET}_3)]$ with alkynyllithium reagents. Thus, when treated with $\text{LiC}\equiv\text{CR}$ (R = Ph (**a**), ^tBu (**b**),

(15) (a) *Comprehensive Organometallic Chemistry II*; Atwood, J. D., Vol. Ed.; Wilkinson, G., Stone, F. G. A., Abel, E. W., Eds.; Elsevier: Oxford, U.K., 1995; Vol. 8. For some representative recent reports see: (b) Werner, H.; Wiedemann, R.; Steinert, P.; Wolf, J. *Chem. Eur. J.* **1997**, *3*, 127; **1996**, *2*, 561. (c) Chi, Ch. S.; Lee, H.; Oh, M. *Organometallics* **1997**, *16*, 816. (d) Werner, H.; Gever, O.; Haquette, P. *Organometallics* **1997**, *16*, 803. (e) Cooper, A. C.; Huffman, J. C.; Caulton, K. G. *Organometallics* **1997**, *16*, 1974. (f) Esteruelas, M. A.; Olivan, M.; Oro, L. A. *Organometallics* **1996**, *15*, 814. (g) Werner, H.; Gevert, O.; Steiner, P.; Wolf, J. *Organometallics* **1995**, *14*, 1786. (h) Tykwinski, R. R.; Stang, P. J. *Organometallics* **1994**, *13*, 3203. (i) Kishimoto, Y.; Eckerle, P.; Miyatake, T.; Ikariya, T.; Noyori, R. *J. Am. Chem. Soc.* **1994**, *116*, 12131. (j) Deyder, E.; Menu, M. J.; Dartiguenave, M.; Dartiguenave, Y. *J. Organomet. Chem.* **1994**, *479*, 55. (k) Bianchini, C.; Meli, A.; Peruzzini, M.; Vacca, A.; Laschi, F.; Zanollo, P.; Ottaviani, F. M. *Organometallics* **1990**, *9*, 360. (l) Werner, H.; Baum, M.; Schneider, D.; Windmüller, B. *Organometallics* **1994**, *13*, 1089. See also ref 32.

(16) (a) Werner, H.; Wolf, J.; Garcia Alonso, F. J.; Ziegler, M. L.; Serhadli, O. *J. Organomet. Chem.* **1987**, *336*, 397. (b) Lamata, M. P.; San José, E.; Carmona, D.; Lahoz, F. J.; Atencio, R.; Oro, L. A. *Organometallics* **1996**, *15*, 4852. (c) Carmona, D.; Lahoz, F. J.; Atencio, R.; Oro, L. A.; Lamata, M. P.; San José, E. *Tetrahedron: Asymmetry* **1993**, *4*, 1425.

(17) Meyer, T. Y.; Woerpel, K. A.; Novak, B. M.; Bergman, R. G. *J. Am. Chem. Soc.* **1994**, *116*, 10290.

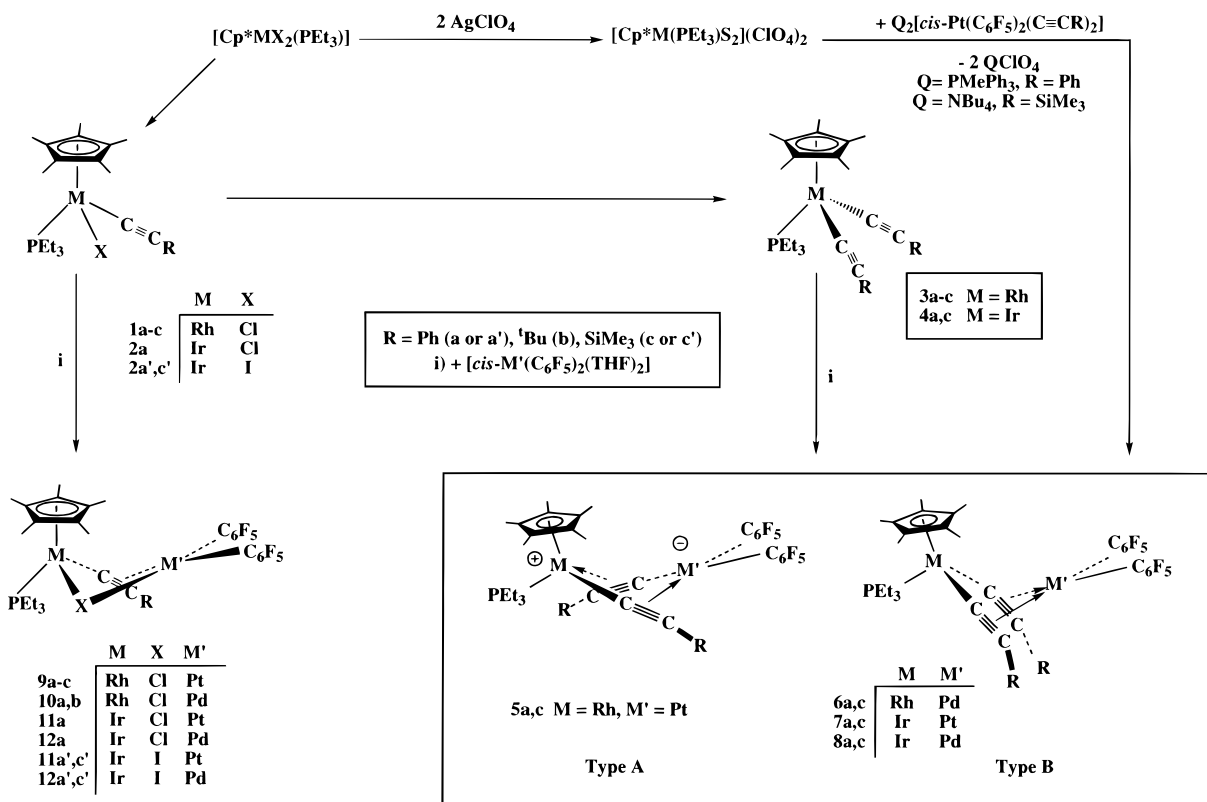
(18) Moreto, J.; Maruya, K.-I.; Bailey, P. M.; Maitlis, P. M. *J. Chem. Soc., Dalton Trans.* **1982**, 1341.

(19) Kang, J. W.; Moseley, K.; Maitlis, P. M. *J. Am. Chem. Soc.* **1969**, *91*, 5970.

(13) (a) Usón, R.; Forniés, J.; Tomás, M.; Menjón, B.; Fortuño, C.; Welch, A. J.; Smith, D. E. *J. Chem. Soc., Dalton Trans.* **1993**, 275. (b) Forniés, J.; Gómez-Saso, M. A.; Lalinde, E.; Martínez, F.; Moreno, M. T. *Organometallics* **1992**, *11*, 2873. (c) Forniés, J.; Lalinde, E.; Martín, A.; Moreno, M. T. *J. Chem. Soc., Dalton Trans.* **1994**, 135. (d) Berenguer, J. R.; Forniés, J.; Lalinde, E.; Martínez, F. *J. Organomet. Chem.* **1994**, *470*, C15. (e) *Organometallics* **1996**, *15*, 4537. (f) Waldbach, T. A.; van Eldik, R.; van Rooyen, P. H.; Lotz, S. *Organometallics* **1997**, *16*, 4056.

(14) Berenguer, J. R.; Forniés, J.; Lalinde, E.; Martínez, F. *J. Chem. Soc., Chem. Commun.* **1995**, 1227.

Scheme 1



SiMe₃ (c) the dichlororhodium complex [Cp*RhCl₂(PEt₃)] afforded the monoalkynyl derivatives [Cp*Rh(C≡CR)Cl(PEt₃)] (**1a–c**) (Scheme 1). Optimal reaction conditions require the use of an excess of LiC≡CR (Rh/Li = 1/4 (Ph), 1/6 (^tBu)), a low temperature (–20 °C), and short reaction times. After the reaction mixture for R = ^tBu is quenched for 10 min, the monoalkynyl complex **1b** is isolated as a pure orange solid, although in low yield (33%) due to its high solubility in the usual solvents, even in hexane. However, despite many attempts with different reaction times complex **1a** can only be obtained as an oily sample containing small amounts of **3a** (~14%) and [Cp*RhCl₂(PEt₃)] (~12%) by quenching the reaction for 2 min. This impure sample was further employed to prepare the heterobridged derivatives **9a** and **10a**. It should be noted that, in general, when the reactions occur at room temperature and/or with prolonged reaction times the monoalkynyl compounds are rapidly consumed and the bis(alkynyl) species [Cp*Rh(C≡CR)₂(PEt₃)] (**3a–c**) are easily formed. On the other hand, when [Cp*RhCl₂(PEt₃)] is treated with stoichiometric amounts of LiC≡CR (1 or 2 equiv), the reactions do not go to completion and variable mixtures (depending on the reaction times) of **1** and **3** along with the dichloride precursor are invariably formed.

In the reaction of [Cp*RhCl₂(PEt₃)] with LiC≡CSiMe₃ the displacement of the second chloride on **1c** is so fast that, despite many attempts, we have not succeeded in obtaining pure **1c**. Thus, when [Cp*RhCl₂(PEt₃)] is stirred at low temperature (–20 °C) with 4 equiv of LiC≡CSiMe₃ for only 2 min, the bis(alkynyl) species [Cp*Rh(C≡CSiMe₃)₂(PEt₃)] (**3c**) is formed along with the mono(alkynyl)rhodium complex [Cp*Rh(C≡CSiMe₃)Cl(PEt₃)] (**1c**). Following workup, an orange oil is

obtained for which the ¹H, ³¹P and ¹³C NMR spectra reveal that the ratio **1c**:**3c** is 2:1. The formation of a mixture of **1c** and **3c** (and also **1a** and **3a**) is well-rationalized in terms of competing chloride–alkynyl exchange between the formed **1c** and [Cp*RhCl₂(PEt₃)]. Complex **3c** is prepared pure as a red oil in high yield (87%) after workup of the reaction mixture of [Cp*RhCl₂(PEt₃)] with LiC≡CSiMe₃ (6.5 equiv) stirred for 30 min at room temperature. In contrast, the bis(alkynyl) derivatives **3a** (R = Ph) and **3b** (R = ^tBu) are obtained (see Experimental Section) as brown air-stable solids in moderate yield (69%, **3a**; 47%, **3b**). Analyses, mass spectra (FAB+), and NMR (¹H, ³¹P{¹H}, and ¹³C{¹H}) spectral data are reported in the Experimental Section and selected IR data in Table 1. The most noticeable absorptions in the IR spectra of **1** and **3** are those corresponding to the ν(C≡C) vibrations which appear in the range 2033 (**3c**)–2110 cm^{–1} (**3b**), confirming terminal coordination of these ligands. As expected, the ³¹P NMR spectra show a doublet due to ¹⁰³Rh–³¹P coupling. Interestingly, the gradual substitution of the chlorides by C≡CR ligands causes a gradual shift of the signals to lower field (δ 37.2 (**3a**), 37.3 (**3b**), 36.6 (**3c**) vs 32.9 (**1a**), 32.6 (**1b,c**); δ 28.0 [Cp*RhCl₂(PEt₃)]). In the ¹³C NMR spectra, the signals of the alkynyl carbons are found in the typical chemical shift ranges, split into a doublet of doublets due to rhodium and phosphorus coupling. Assignment is based on the stronger couplings that are assumed to occur with the σ-bond α-carbon (¹J_{Rh–C_α} = 49–54 Hz, ²J_{31P–C_α} = 28–38.1 Hz vs ²J_{103Rh–C_β} = 7.8–10.3 Hz and ³J_{31P–C_β} = 2.7–3 Hz).

The reactions between [Cp*IrCl₂(PEt₃)] or [Cp*IrI₂(PEt₃)] and LiC≡CR have also been investigated. Depending on the reaction time, treatment of [Cp*IrX₂(PEt₃)] (X = Cl, I) with an excess of LiC≡CSiMe₃ (10

Table 1. IR Data (cm⁻¹) for Complexes 1–12

mononuclear		dinuclear		
[M]X(C≡CR) ^a	ν(C≡C)	[M](μ-X)(μ-C≡CR)[M'] ^b	ν(C≡C)	Δν(C≡C) (cm ⁻¹)
[Rh]Cl(C≡CPh) (1a)	2105 (s)	[Rh](μ-Cl)(μ-η ¹ :η ² -C≡CPh)[Pt] (9a)	2039 (m)	66
[Rh]Cl(C≡C ^t Bu) (1b)	2108 (vs)	[Rh](μ-Cl)(μ-η ¹ :η ² -C≡CPh)[Pd] (10a)	2059 (m)	46
[Rh]Cl(C≡CSiMe ₃) (1c)	2035 (vs)	[Rh](μ-Cl)(μ-η ¹ :η ² -C≡C ^t Bu)[Pt] (9b)	1992 (w)	116
[Ir]Cl(C≡CPh) (2a)	2102 (s)	[Rh](μ-Cl)(μ-η ¹ :η ² -C≡C ^t Bu)[Pd] (10b)	2026 (m)	82
[Ir]I(C≡CPh) (2a')	2105 (vs)	[Rh](μ-Cl)(μ-η ¹ :η ² -C≡CSiMe ₃)[Pt] (9c)	1940 (s)	95
[Ir]I(C≡CSiMe ₃) (2c')	2038 (vs)	[Ir](μ-Cl)(μ-η ¹ :η ² -C≡CPh)[Pt] (11a)	2042 (s)	60
[Rh](C≡CPh) ₂ (3a)	2107 (vs)	[Ir](μ-Cl)(μ-η ¹ :η ² -C≡CPh)[Pd] (12a)	2062 (s)	40
[Rh](C≡C ^t Bu) ₂ (3b)	2155 (sh), 2110 (s)	[Ir](μ-I)(μ-η ¹ :η ² -C≡CPh)[Pt] (11a')	2021 (m), 1985 (w)	84, 120 (average 102)
[Rh](C≡CSiMe ₃) ₂ (3c)	2033 (s br)	[Ir](μ-I)(μ-η ¹ :η ² -C≡CPh)[Pd] (12a')	2046 (s)	59
[Ir](C≡CPh) ₂ (4a)	2118, 2108 (vs)	[Ir](μ-I)(μ-η ¹ :η ² -C≡CSiMe ₃)[Pt] (11c')	1921 (s)	117
[Ir](C≡CSiMe ₃) ₂ (4c)	2035 (s) ^d	[Ir](μ-I)(μ-η ¹ :η ² -C≡CSiMe ₃)[Pd] (12c')	1940 (vs)	98
		[Rh](μ-η ¹ :η ² -C ₂ Ph)(μ-η ² :η ¹ C ₂ Ph)[Pt] (5a) ^c	1900 (s)	207
		[Rh](μ-η ¹ :η ² -C≡CPh) ₂ [Pd] (6a)	2065 (s)	42
		[Rh](μ-η ¹ :η ² -C ₂ SiMe ₃)(μ-η ² :η ¹ C ₂ SiMe ₃)[Pt] (5c)	1905, 1867 (vs)	128, 166 (average 147)
		[Rh](μ-η ¹ :η ² -C≡CSiMe ₃) ₂ [Pd] (6c)	1963 (s br)	70
		[Ir](μ-η ¹ :η ² -C≡CPh) ₂ [Pt] (7a)	2031 (s), 1971 (m)	87, 137 (average 112)
		[Ir](μ-η ¹ :η ² -C≡CPh) ₂ [Pd] (8a)	2068 (s)	50, 40 (average 45)
		[Ir](μ-η ¹ :η ² -C≡CSiMe ₃) ₂ [Pt] (7c)	1927, 1905 (s)	108, 130 (average 119)
		[Ir](μ-η ¹ :η ² -C≡CSiMe ₃) ₂ [Pd] (8c)	1963, 1943 (s)	72, 92 (average 82)

^a [M] = [MCp*(PEt₃)]. ^b [M'] = [M'(C₆F₅)₂]. ^c Two very weak bands at 2018 and 1988 cm⁻¹ are also observed. ^d Two shoulders at 2049 and 2026 cm⁻¹ are also observed.

equiv for X = Cl or 15 equiv for X = I) in thf results in the formation of [Cp*Ir(C≡CSiMe₃)X(PEt₃)] (X = Cl, **2c**; X = I, **2c'**) or the corresponding bis(alkynyl) derivative [Cp*Ir(C≡CSiMe₃)₂(PEt₃)] (**4c**). The reaction was monitored by ³¹P NMR, showing that, as expected, the formation of **2c, c'** precedes that of **4c**. Over a period of 1 h for X = Cl or 4 h for X = I the conversion of [Cp*IrX₂(PEt₃)] to **4c** is nearly complete and after workup (see Experimental Section) **4c** can be isolated as a solid in high yield, 85–90%. The monoalkynyl derivative **2c'** is obtained in 94% yield by quenching the reaction mixture for no more than 50 min. However, although the mono(alkynyl) chloro derivative **2c** was clearly observed by ³¹P NMR spectroscopy (δ -7.8), in the course of the final formation of **4c**, this complex could not be separated pure from the reaction mixture, which always contains variable amounts of the dichloride precursor and **4c**. All attempts to prepare the analogous *tert*-butyl derivatives **2b** and **4b** by this synthetic route failed. In addition, in the reaction of [Cp*IrCl₂(PEt₃)] with LiC≡CPh under different conditions (excess of LiC≡CPh and/or short or prolonged reaction times; see Experimental Section) inseparable mixtures of **2a** and **4a** are invariably obtained.

The synthesis of [Cp*Ir(C≡CPh)Cl(PEt₃)] (**2a**) is, however, possible by the reaction of [Cp*IrCl₂(PEt₃)] with an excess of [AgC≡CPh]_n (2 equiv) in CH₂Cl₂. This reaction occurs in a straightforward manner within 3–4 h at room temperature. At this stage of the reaction the transformation of [Cp*IrCl₂(PEt₃)] into **2a** is nearly complete and only traces of **4a** can be detected (³¹P NMR) (see Experimental Section). Longer reaction times cause a slow conversion of **2a** into **4a**, but concomitant formation of a heteropolynuclear iridium–silver complex is also observed (δ ³¹P -5.9), probably due to the partial redissolution of the AgCl formed. The interaction of AgCl with bis(alkynyl) derivatives^{2c,20} and the formation of heteropolynuclear alkynyl-containing silver compounds by treatment of transition-metal

derivatives with the polymeric [AgC≡CR]_n substrates have been previously reported.²¹ In our system, the only signal observed (δ -5.9, s) in the final ³¹P NMR spectrum together with that corresponding to complex **4a** (δ -8.5) (signal ratio ~1:2) is also observed by monitoring a CDCl₃ solution of **4a** treated with an excess of AgCl(s) (Ir:Ag = 1:3). In both cases the system seems to reach the same ratio between both signals, thus indicating that a possible equilibrium between **4a**, AgCl(s), and the heteropolynuclear Ir–Ag complex is probably occurring. Further attempts to separate this equilibrium mixture were unsuccessful. However, the formation of pure **4a** was achieved by using the corresponding diiodide derivative [Cp*IrI₂(PEt₃)] as the starting material and either of the alkynylation agents (LiC≡CPh or AgC≡CPh). Thus, the reaction of [Cp*IrI₂(PEt₃)] with a considerable excess of LiC≡CPh (molar ratio Ir:Li = 1:15) produces, after ca. 6.5 h of stirring, the bis(alkynyl) complex **4a** in very high yield (~90%). The mono(alkynyl) iodide derivative **2a'** is observed during the course of the reaction, but it is always present along with notable amounts of **4a** and the diiodide starting material, which prevents its isolation in a pure form. Complex **4a** can also be obtained by stirring [Cp*IrI₂(PEt₃)] with an excess of [AgC≡CPh]_n (3.8 equiv) for 4 days. In this way, the expected bis(alkynyl) compound is easily obtained as a beige solid in high yield (78%). As expected, the complex is also formed through the corresponding mono(alkynyl) iodide derivative [Cp*Ir(C≡CPh)I(PEt₃)] (**2a'**) as an intermediate, which is easily identified (³¹P NMR) in the course of the reaction. However, using this alternative route compound **2a'** can also be isolated as an orange solid in

(21) (a) Abu Salah, D. M.; Bruce, M. I. *J. Chem. Soc., Chem. Commun.* **1974**, 688; *Aust. J. Chem.* **1977**, *30*, 2639. (b) Churchill, M. R.; De Boer, B. G. *Inorg. Chem.* **1975**, *14*, 2630. (c) Espinet, P.; Forníes, J.; Martínez, F.; Tomás, M.; Lalinde, E.; Moreno, M. T.; Ruiz, A.; Welch, A. J. *J. Chem. Soc., Dalton Trans.* **1990**, 791. (d) Espinet, P.; Forníes, J.; Martínez, F.; Sotés, M.; Lalinde, E.; Moreno, M. T.; Ruiz, A.; Welch, A. J. *J. Organomet. Chem.* **1991**, *403*, 253. (e) Forníes, J.; Gómez-Saso, M. A.; Martínez, F.; Lalinde, E.; Moreno, M. T.; Welch, A. J. *New J. Chem.* **1992**, *16*, 483. (f) Sladkov, A. M.; Gold'ing, I. R. *Russ. Chem. Rev. (Engl. Transl.)* **1979**, *48*, 869.

(20) Forníes, J.; Lalinde, E.; Martín, A.; Moreno, M. T. *J. Organomet. Chem.* **1995**, *490*, 179.

moderate yield (56%) from the resulting final reaction mixture obtained by refluxing $[\text{Cp}^*\text{IrI}_2(\text{PET}_3)]$ with an excess of $[\text{AgC}\equiv\text{CPh}]_n$ (3 equiv) in CH_2Cl_2 over ca. 90 min (see Experimental Section for details). Unfortunately, all attempts to prepare the *tert*-butyl derivatives **2b** and **4b** using this alternative synthetic route were fruitless. The reaction of $[\text{AgC}\equiv\text{C}^t\text{Bu}]_n$ with $[\text{Cp}^*\text{IrX}_2(\text{PET}_3)]$ ($\text{X} = \text{Cl}, \text{I}$) only yields heteropolynuclear iridium–silver complexes, and a mixture of compounds, which we have not been able to separate, were also obtained by using an excess of the (3,3-dimethylbutynyl)lithium derivative. These iridium complexes **2a, a', c'** and **4a, c** have been characterized by analytical and spectroscopic means (see Table 1 and Experimental Section for details). The most striking spectroscopic feature is that the $^31\text{P}\{\text{H}\}$ NMR spectra of **2** and **4**, unlike the Rh analogues **1** and **3**, show a singlet resonance at fields higher than that shown by the corresponding dichloride precursor; in addition, the gradual substitution of the chloride by alkynyl ligands also produces a gradual phosphorus shift displacement to lower frequency ($\delta -8.5$ (**4a**) -9.2 (**4c**) vs -7.3 (**2a**), -7.8 (**2c**); $\delta -6.3$ for $[\text{Cp}^*\text{IrCl}_2(\text{PET}_3)]$). The opposite situation is found in the mono(alkynyl) iodide derivatives **2a', c'**, which show a singlet ($\delta -12.7$ (**2a'**), -13.2 (**2c'**)) at frequency higher than that observed for $[\text{Cp}^*\text{IrI}_2(\text{PET}_3)]$ ($\delta -19.7$).

Heterodinuclear Derivatives. The preparation of either bis(alkynyl)- or halide–alkynyl-bridged dinuclear complexes was easily accomplished using the bridge-assisted synthetic methodology.

Thus, the reaction of mono(alkynyl) mononuclear complexes **1a, b** and **2a, a', c'** with an equimolar amount of $[\text{cis-Pt}(\text{C}_6\text{F}_5)_2(\text{thf})_2]$ in CH_2Cl_2 at room temperature results in the formation of neutral heterobridged platinum complexes $[(\text{PET}_3)\text{Cp}^*\text{M}(\mu\text{-C}\equiv\text{CR})(\mu\text{-X})\text{Pt}(\text{C}_6\text{F}_5)_2]$ (**9a, b**, $\text{M} = \text{Rh}$, $\text{X} = \text{Cl}$; **11a**, $\text{M} = \text{Ir}$, $\text{X} = \text{Cl}$; **11a', c'**, $\text{M} = \text{Ir}$, $\text{X} = \text{I}$) (Scheme 1). The analogous reaction of **1a, b** and **2a, a', c'** with $[\text{cis-Pd}(\text{C}_6\text{F}_5)_2(\text{thf})_2]$ (molar ratio 1:1) in CH_2Cl_2 , but at lower temperature (-20°C), gives the corresponding hetero ($\mu\text{-C}\equiv\text{CR})(\mu\text{-X})$ Rh–Pd (**10a, b**, $\text{X} = \text{Cl}$) and Ir–Pd (**12a**, $\text{X} = \text{Cl}$; **12a', c'**, $\text{X} = \text{I}$) compounds, respectively. Similarly, the reaction of the bis(alkynyl) derivatives $[\text{Cp}^*\text{M}(\text{C}\equiv\text{CR})_2(\text{PET}_3)]$ (**3a, c**, $\text{M} = \text{Rh}$; **4a, c**, $\text{M} = \text{Ir}$) with $[\text{cis-M}'(\text{C}_6\text{F}_5)_2(\text{thf})_2]$ ($\text{M}' = \text{Pt}, \text{Pd}$) (1:1) in CH_2Cl_2 , at room ($\text{M}' = \text{Pt}$) or low (-20°C , $\text{M}' = \text{Pd}$) temperature (diethyl ether for **6a**) results in the formation of the heterodinuclear homobridged $[(\text{PET}_3)\text{Cp}^*\text{M}(\mu\text{-C}\equiv\text{CR})_2\text{M}'(\text{C}_6\text{F}_5)_2]$ (**5a, c** (Rh–Pt), **6a, c** (Rh–Pd), **7a, c** (Ir–Pt), and **8a, c** (Ir–Pd)) complexes.

As expected, when the inseparable **1c** + **3c** mixture (ratio 2:1) is treated with 1 equiv of $[\text{cis-Pt}(\text{C}_6\text{F}_5)_2(\text{thf})_2]$ in CH_2Cl_2 at room temperature, a similar mixture of the corresponding hetero- (**9c**) and homobridged (**5c**) dinuclear complexes is produced. Due to similar solubilities, all attempts (see Experimental Section) to obtain **9c** as a pure complex from the mixture (**9c**:**5c** = 4:1) obtained after the usual workup were unsuccessful; it is, however, easily characterized by spectroscopic means in solution (see below and Experimental Section). The reaction between the bis(*tert*-butyl) derivative $[\text{Cp}^*\text{Rh}(\text{C}\equiv\text{C}^t\text{Bu})_2(\text{PET}_3)]$ (**1b**) and $[\text{cis-Pt}(\text{C}_6\text{F}_5)_2(\text{thf})_2]$ in CH_2Cl_2 produces a very dark green solution that with

the usual workup rapidly becomes brown, from which no definite product could be obtained.

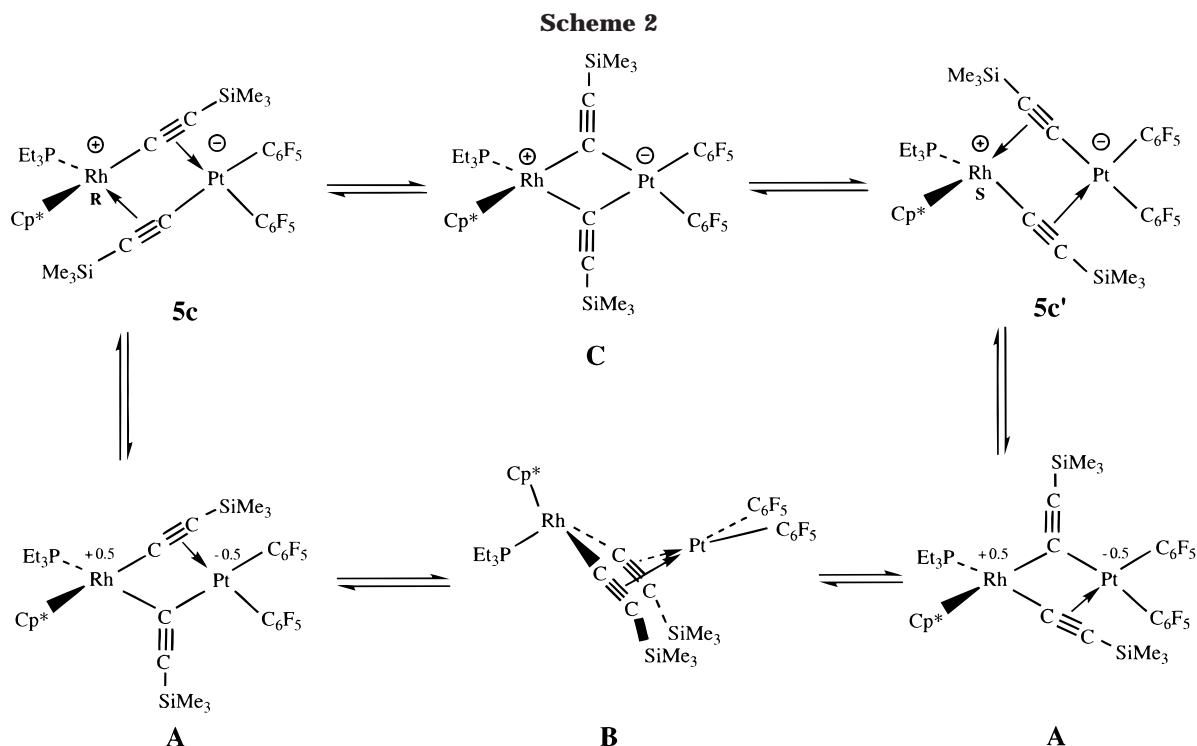
As shown in Scheme 1, there is a second route to obtaining the heterodinuclear platinum derivatives with a double-alkynyl bridging system. Thus, complexes **5** and **7** can be prepared by reacting the anionic $\text{Q}_2[\text{cis-Pt}(\text{C}_6\text{F}_5)_2(\text{C}\equiv\text{CR})_2]$ ($\text{R} = \text{Ph}$, $\text{Q} = \text{PMePh}_3$; $\text{R} = \text{SiMe}_3$, $\text{Q} = \text{NBu}_4$) and the dicationic bis(solvento) species $[\text{Cp}^*\text{M}(\text{PET}_3)(\text{acetone})_2](\text{ClO}_4)_2$, prepared in situ from $[\text{Cp}^*\text{MCl}_2(\text{PET}_3)]$ and 2 equiv of AgClO_4 in acetone. Although yields do not vary very much using either of the two routes, the first synthetic route is preferred due to the absence of QClO_4 in the reaction mixtures. Unfortunately, when using the second route the reactions between $(\text{NBu}_4)_2[\text{cis-Pt}(\text{C}_6\text{F}_5)_2(\text{C}\equiv\text{C}^t\text{Bu})_2]$ and the solvento species $[\text{Cp}^*\text{M}(\text{PET}_3)(\text{acetone})_2](\text{ClO}_4)_2$ also produce intractable solution mixtures (NMR spectroscopy) from which the expected dimers could not be obtained.

These heterodinuclear complexes have different properties. Thus, heteronuclear Ir–Pt (**7a, c**, **11a, a', c'**) and Ir–Pd (**8a, c**, **12a, a', c'**) complexes are yellow, whereas the corresponding rhodium derivatives Rh–Pt (**5a, c**, **9a, b**) or Rh–Pd (**6a, c**, **10a, b**) are orange. Moreover, although all compounds are air-stable in the solid state, the phenylethynyl derivatives slowly decompose in solution. In particular, the decomposition of the (phenylethynyl)rhodium-containing complexes **5a**, **6a**, **9a**, and **10a** in solution is very fast even at low temperature (-50°C). Finally, the double-alkynyl-bridged complexes (**5–8**) are considerably more soluble than the heterobridged $\mu\text{-C}\equiv\text{CR}-\mu\text{-X}$ compounds **9–12**.

All of the complexes have been fully characterized by analytical (except **9c**) and spectral means, and the molecular structures of **5c**, **7a, c**, **8a**, **9b**, and **12a** have been unambiguously confirmed by X-ray diffraction (see Experimental Section for details).

Evidence of the formation of these heterodinuclear complexes with alkynyl bridging ligands is obtained from the IR spectra, which show, in each case, that the alkyne $\nu(\text{C}\equiv\text{C})$ is shifted to smaller wavenumbers. As can be seen in Table 1, the observed shift, $\Delta\nu(\text{C}\equiv\text{C})$ (cm^{-1}), in the heterometallic platinum complexes is always larger than in related palladium compounds both for doubly alkynyl bridging derivatives (**5–8**) and for heterobridged species (**9–12**). This spectroscopic fact indicates that, in line with previous observations,^{12d} the η^2 -alkyne–metal interaction is stronger in platinum than in palladium complexes.

The ^1H NMR spectra of the homobridged $[\text{Cp}^*\text{M}(\mu\text{-C}\equiv\text{CSiMe}_3)_2\text{M}'(\text{C}_6\text{F}_5)_2]$ (**5c–8c**), both at low temperature (-50°C) and at room temperature, only show one type of alkynyl environment. As in its solid state complex **5c** exhibits an unsymmetrical formal zwitterionic structure, $[(\text{PET}_3)\text{Cp}^*\text{Rh}^+(\mu\text{-}\sigma\text{:}\eta^2\text{-C}\equiv\text{CSiMe}_3)(\mu\text{-}\eta^2\text{:}\sigma\text{-C}\equiv\text{CSiMe}_3)\text{Pt}^-(\text{C}_6\text{F}_5)_2]$, (see below), for this complex, the spectra can only be explained by assuming a rapid exchange between **5c** and **5c'** enantiomers even at a very low (-90°C) temperature (Scheme 2). Fast migration of the alkynyl ligands between the metal centers may take place involving the formation of symmetrical chelating **B** type intermediates which, in turn, are easily accessible through asymmetric **A** type species with double-alkynyl bridging systems (Scheme 2). Similar observations have been previously observed in the case



of related homonuclear $[(C_5H_4^tBu)_2Zr(\mu-\sigma:\eta^2-C\equiv CR)(\mu-\eta^2:\sigma-C\equiv CR)Zr(C_5H_4^tBu)_2]$ ^{11a} and heteronuclear $[Cp_2Ti(\mu-\sigma:\eta^2-C\equiv CSiMe_3)(\mu-\eta^2:\sigma-C\equiv CSiMe_3)Ni(PPh_3)]$ ^{8d} compounds, which had been found in equilibrium at low temperature with the corresponding symmetrical **B** type species. We also noted that the formation of a very asymmetric double-alkynyl **A** type bridging system, approximately halfway between **5c** and **B** (**IV**; Chart 1), has been recently found in the mixed complex $[Cp_2Ti(\mu-\sigma-C\equiv C^tBu)(\mu-\sigma:\eta^2-X\equiv C^tBu)Pt(PPh_3)]$.^{11d} Notwithstanding, the change could occur directly through the $\mu,\sigma-C\equiv CSiMe_3$ intermediate **C**. In fact, we have also demonstrated that this type of species can also be stable. The X-ray study of $[Cp_2Ti(\mu-C\equiv C^tBu)_2Pt(C_6F_5)_2]$ reveals that, although the alkynyl ligands were initially σ -bonded to the Ti center, the $\mu,\sigma-C\equiv C^tBu$ groups are tilted in this dimer in such a way that the σ -bonding orbitals point more to the Pt atom.^{10b}

Heterobridged $[(PET_3)Cp^*M(\mu-C\equiv CR)(\mu-X)M'(C_6F_5)_2]$ complexes **9–12** proved not to be soluble enough for ¹³C NMR analysis and the spectra of (phenylethynyl)-rhodium derivatives **5a** and **6a** and those of the palladium complexes **6c** and **8c** could not be obtained due to their very low stability in solution. The platinum derivatives **5c** and **7c** ($R = SiMe_3$) exhibit, in the low-temperature ¹³C NMR spectra, the expected signals due to Cp* and PET₃ ligands, while SiMe₃ units appear as a singlet at δ 1.53 for **5c** and δ 0.92 for **7c**, respectively, once again indicating that both C \equiv CR units are equivalent. However, despite prolonged accumulation and probably due to their limited solubility at low temperature, the alkynyl carbon signals could not be located for **5c** and only an ill-defined resonance at 93.77 ppm (C_α or C_β) is seen for **7c**. Complexes **7a** and **8a** are considerably more soluble and, in line with the structures found in the solid state, complexation of the "Pt-(C₆F₅)₂" and "Pd(C₆F₅)₂" units by the bis(phenylethynyl)-iridium fragment is clearly shown by the upfield ¹³C chemical shift of the C_α carbon atoms ($\delta(C_\alpha/C_\beta)$ 55.3/

98.0 (**7a**) and 51.29/100.52 (**8a**) vs 80.2/98.7 (**4a**). Similar upfield shifts of the C_α atoms have been previously observed upon complexation of a d⁸ metal center (Pt, Pd, Rh(I), Ir(I)) by a bis(alkynyl) $[M](C\equiv CR)_2$ fragment.^{13e,22} The C_β resonances seem to be less affected, and in general, they do not show such a clear trend.

The asymmetry of the heterobridged compounds **9–12** is clearly reflected in the ¹⁹F NMR spectra, which, in each case, show the expected two sets of five signals confirming the presence of two nonequivalent rigid C₆F₅ rings (two AFMRX systems). The room-temperature NMR data (¹H, ³¹P, and ¹⁹F) reveal no evidence of possible conformers and, unfortunately, they are not soluble enough (except **11c'**, **12c'**) for low-temperature studies. For **11c'** and **12c'** similar patterns of ¹H, ³¹P, and ¹⁹F NMR were found at $-50^\circ C$. Complexes **9b** and **12a** crystallize adopting a bent disposition, and the conformer found (see below) is that which places the "M'(C₆F₅)₂" unit *endo* to the Cp* ligand. However, although it is unlikely, a rapid interconversion of conformers in solution cannot be excluded.

As we will see later, solid-state structures of Ph-substituted complexes **7a** and **8a** show that the iridium fragment $[Cp^*Ir(C\equiv CPh)_2(PET_3)]$ is chelating the "*cis*-M'(C₆F₅)₂" unit with the chelated metal center (Pt, **7a**; Pd, **8a**) located in both complexes out of the 3-irida-1,4-diyne plane (IrC₄), thus giving bent IrC₄M cores. Consequently, two conformers with either the PET₃ or the Cp* ring toward the M'(C₆F₅)₂ unit are possible but the ³¹P NMR spectra of **7a** and **8a** (and also of **5–8**) display only one singlet (see above) at all temperatures, thus suggesting the presence, in solution, of only one isomer or a rapid interconversion of isomers even at low temperature. In **7a** and **8a** (and also in **7c**, **9b**, **12a**, and even **5c**) the formation of the conformer with the

$M'(C_6F_5)_2$ fragment oriented toward the Cp^* ring (see Figures 1–6) is observed in the solid state. Therefore, in **7a** and **8a** both C_6F_5 groups are equivalent but the halves on each ring must be inequivalent. It should be also noted that a possible rapid interconversion of isomers (fast inversion of the central IrC_4M core), which cannot be excluded, does not exchange the halves of the C_6F_5 ring. Accordingly, both complexes exhibit the expected five signals of equal intensity in the ^{19}F NMR spectra at low temperature ($-50\text{ }^\circ\text{C}$), thus confirming a restricted rotation of the C_6F_5 groups along the $M-C$ ($M = Pt, Pd$) bond. Increasing the monitoring temperature resulted in a broadening of the two *ortho* (coalescence up to $45\text{ }^\circ\text{C}$) and two *meta* fluorine resonances in complex **7a**. In contrast, no noticeable change was observed in the Pd complex **8a**, which is rigid up to room temperature (its low stability in solution precluded observation at higher temperatures). In **7a** the most simple dynamic process that would produce the exchange of the halves of the C_6F_5 rings is, of course, their free rotation along the $Pt-C$ bond with or without alkyne– Pt breaking. Another less likely possibility would be dissociation of the $Pt(C_6F_5)_2$ unit. The influence of different factors on the rotation of C_6F_5 rings in (pentafluorophenyl)palladium and -platinum complexes has been recently discussed.²³ If our assumption is correct, our results seem to indicate a relatively faster rotation of C_6F_5 rings in **7a** compared to that in compound **8a**.

Similar behavior was observed in the phenylethynyl $Rh-Pt$ derivative **5a**, which displayed one broad *o*-F (nearly coalesces) and one *m*-F resonance at room temperature that split into two different ones (1:1) at low temperature ($-50\text{ }^\circ\text{C}$), as expected. The analogous $Rh-Pd$ complex **6a** decomposes rapidly in solution at room temperature, and hence, the ^{19}F NMR spectrum was only recorded at $-50\text{ }^\circ\text{C}$, showing one set of five C_6F_5 fluorine signals. Since no suitable crystals of **5a** and **6a** could be obtained due to their rapid decomposition, their structural assignment has been carried out on the basis of available spectroscopic data and is not unequivocal.

For complex **6a** ($Rh-Pd$), the similarity of its ^{19}F NMR spectrum with that of **8a** ($Ir-Pd$) and, especially, the fact that the $\Delta\nu(C\equiv C)$ shift observed in their IR spectra are comparable (42 cm^{-1} in **6a** vs average 45 cm^{-1} in **8a**; Table 1) led us to assume a similar chelating type arrangement of the bis(alkynyl) bridging system. In contrast to this, **5a** ($Rh-Pt$) exhibits a medium $\nu(C\equiv C)$ bond at lower wavenumbers (1900 cm^{-1}) with a shift of 207 cm^{-1} relative to the precursor **3a** (2107 cm^{-1}), which is considerably higher than that observed (average 112 cm^{-1}) in the analogous **7a** ($Ir-Pt$ $\nu(C\equiv C)$ $2031, 1971\text{ cm}^{-1}$). This shift (**3a** \rightarrow **5a** 207 cm^{-1}) is even larger than that observed in **5c** (average 147 cm^{-1}), in which an asymmetrical σ/π doubly alkynyl bridging type **A** (Scheme 2) occurs (X-ray see below). Comparable shifts have been previously observed in related species with similar bonding arrangements of the alkynyl ligands: $[Pt(\mu-C\equiv CR)(C_6F_5)_2]_2^{2-}$ ($\nu(C\equiv C)/\Delta\nu(C\equiv C)$ (cm^{-1}) $1956/\text{average } 133.5$ (Ph), $1923/\text{average } 165$ (^tBu));^{13b} $[Pt(\mu-C\equiv CR)(C_6F_5)(PPh_3)]_2$ ($\nu(C\equiv C)/\Delta\nu(C\equiv C)$ (cm^{-1}) $1963/$

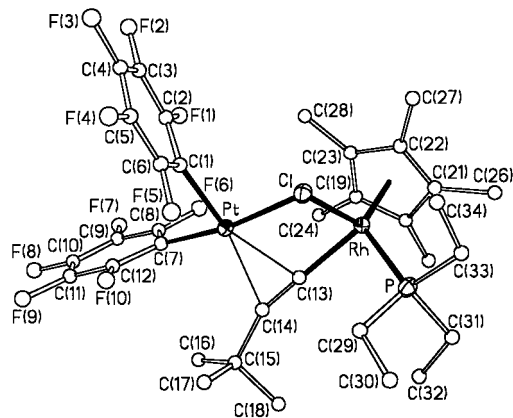


Figure 1. Molecular structure of complex **9b**, showing the atom-numbering scheme. Hydrogen atoms have been omitted for clarity.

146 (Ph), $1986/143$ (^tBu), $1915/125$ ($SiMe_3$)).^{11b} Smaller shifts are always seen upon simple complexation of coordinatively unsaturated ML_n units by 3-metalla-1,4-diyne fragments.^{2c,6,8g,12,13d,e,14} Thus, bearing this in mind, although the formulation is not unambiguous, we favor a σ/π doubly alkynyl bridging system for **5a** similar to that found by X-ray analysis in **5c**.

According to this formulation for **5a** the formal equivalence of both C_6F_5 rings observed (only one *p*-F resonance) and that of the halves on each C_6F_5 at room temperature could be accounted for by assuming that the alkynyl ligands rapidly change places between Rh and Pt (Scheme 2) and that there is a free rotation around the $Pt-C_{ipso}$ bonds. Below room temperature this latter process slows down and only an AFMRX system is seen in the ^{19}F NMR spectrum of **5a** at $-50\text{ }^\circ\text{C}$. The dimer **5c** shows only one set of nonrotating C_6F_5 signals evidencing a alkynyl migration between the metal centers, which seems to be fast even at low temperature. Thus, on cooling the broadening of the room-temperature signals is observed, and this is clearly greater for the low-frequency *o*-F signal ($\delta -116.3$), which disappears in the baseline at $-90\text{ }^\circ\text{C}$.

The chelating type structure of the remaining trimethylsilyl derivatives **6c**, **7c**, and **8c** was supported by a variety of data, including an X-ray diffraction study on **7c**. In particular, the $\Delta\nu(C\equiv C)$ shift (see Table 1) in the IR spectra (70 cm^{-1} , **6c**, $Rh-Pd$; average 119 cm^{-1} , **7c**, $Ir-Pt$; average 82 cm^{-1} , **8c**, $Ir-Pd$) is comparable to those seen in the phenyl-substituted derivatives **7a** (average 112 cm^{-1} $Ir-Pt$) and **8a** (average 45 cm^{-1} $Ir-Pd$) and considerably smaller than that observed in the σ/π asymmetrical dimers **5a** (207 cm^{-1}) and **5c** (average 147 cm^{-1}), respectively. Accordingly, in these derivatives **6c–8c** the two C_6F_5 groups are also seen as equivalent (only one *p*-F signal) even at low temperature (see Experimental Section). The $Ir-Pt$ derivative **7c** exhibits a ^{19}F NMR pattern similar to that of **7a**, displaying two *o*-F (and also *m*-F) broad resonances at room temperature that were well-resolved at $-50\text{ }^\circ\text{C}$ and coalesced at ca. $40\text{ }^\circ\text{C}$. In contrast, for the Pd mixed complexes **6c** and **8c** the rotation of C_6F_5 rings is again restricted at room temperature. No significant changes were observed at low temperature (only sharper *o*-F signals), and the very low stability of these complexes in solution precluded further experiments.

(23) Casares, J. A.; Espinet, P.; Martínez-Illarduya, J. M.; Lin, Y.-S. *Organometallics* **1997**, *16*, 770 and references therein.

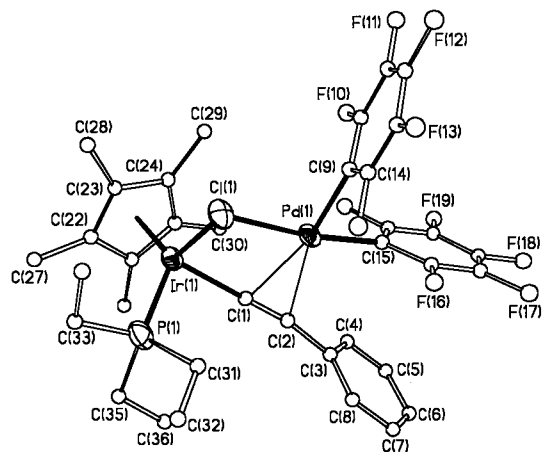


Figure 2. View of the molecular structure of complex **12a**, showing the atom-numbering scheme. Hydrogen atoms have been omitted for clarity.

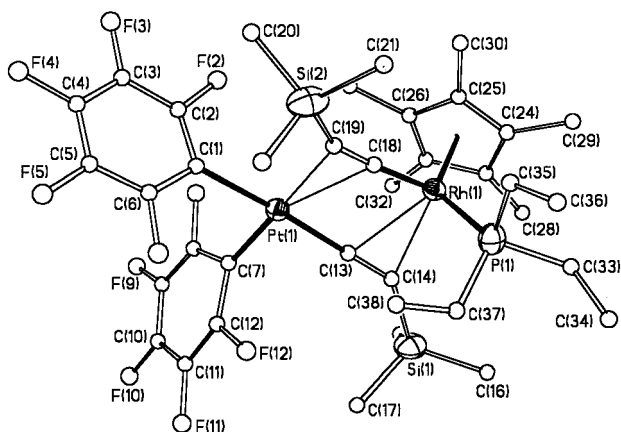


Figure 3. Molecular structure of complex **5c**, showing the atom-numbering scheme. Hydrogen atoms have been omitted for clarity.

Solid-State Structures of Dinuclear Complexes.

X-ray structural studies were carried out on **5c**, **7a,c**, **8a**, **9b**, and **12a** as summarized in Table 2. Refinement, described in the Experimental Section, yielded the structures shown in Figures 1–6. Relevant bond lengths and angles are listed in Table 3. These compounds are new members of the small family of heterometallic $M-M'$ (Rh, Ir–Pt, Pd) complexes which have been structurally characterized to date.²⁴ Figures 1 and 2 show the heterobridged Rh–Pt (**9b**) and Ir–Pd (**12a**) complexes, which consist of $(\text{PET}_3)(\eta^5\text{-C}_5\text{Me}_5)\text{M}$ and $M'(\text{C}_6\text{F}_5)_2$ moieties held together by the $\text{C}\equiv\text{CR}$ bridge and the chloride group. Considering the Cp^* ring to be a single coordination center represented by its centroid, in both molecules (**9b** and **12a**) the Rh and Ir coordina-

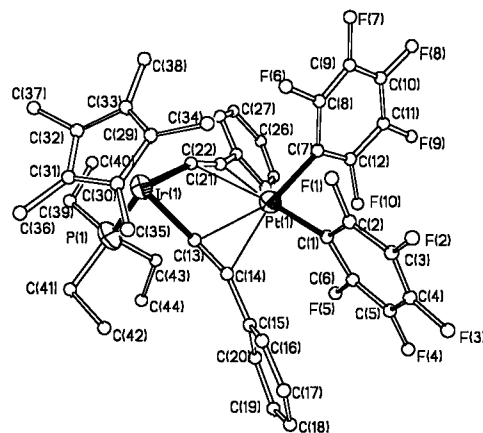


Figure 4. Drawing of the molecular structure of complex **7a**, showing the atom-numbering scheme. Hydrogen atoms have been omitted for clarity.

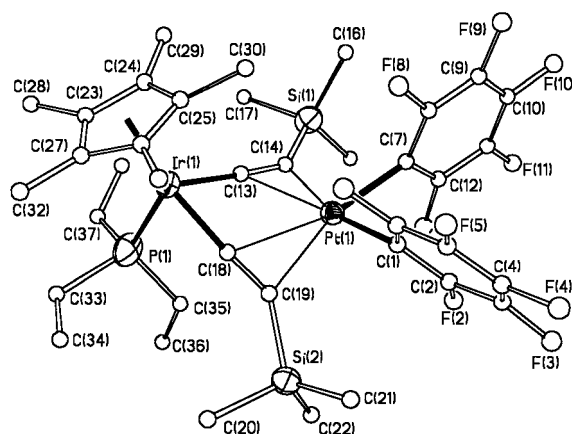


Figure 5. Molecular structure of complex **7c**, showing the atom-numbering scheme. Hydrogen atoms have been omitted for clarity.

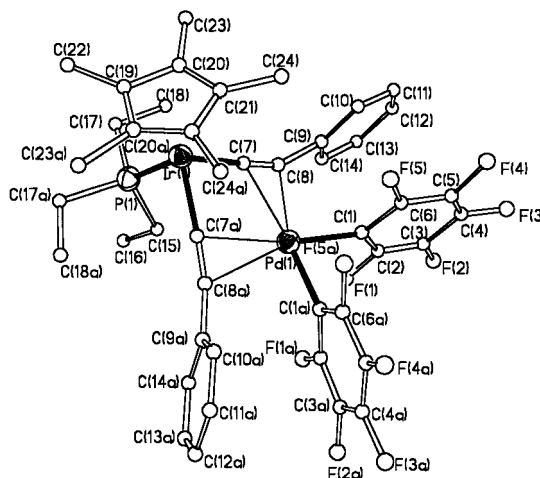


Figure 6. View of the molecular structure of complex **8a**, showing the atom-numbering scheme. Hydrogen atoms have been omitted for clarity.

tion environment can be described as distorted tetrahedral. The deformation from the regular arrangement can be attributed to the bulkiness of the cyclopentadienyl moiety, which forces the other three coordination atoms (phosphorus, carbon, and chlorine) to narrow their interligand angles to less than 90.5° ($80.67(12)$ – $90.23(13)^\circ$, **9b**; $84.4(3)$ – $89.13(10)^\circ$, **12a**), while the corresponding angles with the Cp^* centroid are enlarged

(24) (a) Markham, D. P.; Shaw, B. L.; Thornton-Pett, M. *J. Chem. Soc., Chem. Commun.* **1987**, 1005. (b) Hutton, A. T.; Shebanzadeh, B.; Shaw, B. L. *J. Chem. Soc., Chem. Commun.* **1984**, 549. (c) Albinati, A.; Emge, T. J.; Koetzle, T. F.; Meille, S. V.; Musco, A.; Venanzi, L. M. *Inorg. Chem.* **1986**, *25*, 4821. (d) Lo Schiavo, S.; Rotondo, E.; Bruno, G.; Faraone, F. *Organometallics* **1991**, *10*, 1613 and references therein. (e) Stang, P. J.; Huang, Y. H.; Arif, A. M. *Organometallics* **1992**, *11*, 845; *J. Am. Chem. Soc.* **1990**, *112*, 5648. (f) Stang, P. J.; Huang, Y.-H.; Arif, A. M. *Organometallics* **1992**, *11*, 231. (g) Lu, S.-j.; Wei, F. P.; Wang, X.-d.; Wang, H.-q.; Huang, L.-r. *J. Organomet. Chem.* **1996**, *510*, 7. (h) Tang, Z.; Nomura, Y.; Ishii, Y.; Mizobe, Y.; Hidai, M. *Organometallics* **1997**, *16*, 151. (i) Sipavak, G. J.; Yap, G. P. A.; Puddephatt, R. J. *Polyhedron* **1997**, *16*, 3861 and references therein. (j) Tejel, C.; Shi, Y.-M.; Ciriano, M. A.; Edwards, A. J.; Lahoz, F. J.; Modrego, J.; Oro, L. A. *J. Am. Chem. Soc.* **1997**, *119*, 6679.

Table 2. Crystal Data and Structure Refinement Parameters for Complexes 5c, 7a,c, 8a·0.5CHCl₃, 9b, and 12a^a

	5c	7a	7c	8a·0.5CHCl ₃	9b	12a
empirical formula	C ₃₈ H ₄₈ F ₁₀ PPtRhSi ₂	C ₄₄ H ₄₀ F ₁₀ PPtIr	C ₃₈ H ₄₈ F ₁₀ IrPPtSi ₂	C _{44.5} H _{40.5} Cl _{1.5} F ₁₀ PPdIr	C ₃₄ H ₃₉ ClF ₁₀ PPtRh	C ₃₆ H ₃₅ ClF ₁₀ IrPPd
fw	1280.97	1177.0	1169.20	1148.01	1002.07	1022.66
unit cell dimens						
<i>a</i> (Å)	12.121(2)	19.649(1)	18.555(3)	19.788(4)	19.806(6)	11.472(2)
<i>b</i> (Å)	19.138(3)	10.482(1)	12.514(2)	13.962(3)	10.319(6)	11.528(2)
<i>c</i> (Å)	17.940(30)	20.101(2)	18.372(3)	17.471(3)	19.506(6)	15.392(2)
α (deg)	90	90	90	90	90	102.79(1)
β (deg)	90.55(1)	90	90	90	118.40(3)	104.26(1)
γ (deg)	90	90	90	90	90	104.41(1)
<i>V</i> , (Å ³), <i>Z</i>	4161.4(12)	4041(2), 4	4265.9(12)	4827(2), 4	3506.8(15), 4	1822.1(5)
wavelength (Å)	0.71073	0.71073	0.71073	0.71073	0.71073	0.71073
temp (K)	200	298	200	210	150(1)	200
radiation	graphite monochromated, Mo Kα	graphite monochromated, Mo Kα	graphite monochromated, Mo Kα	graphite monochromated, Mo Kα	graphite monochromated, Mo Kα	graphite monochromated, Mo Kα
cryst syst	monoclinic	orthorhombic	orthorhombic	orthorhombic	monoclinic	triclinic
space group	<i>P2</i> ₁ / <i>n</i>	<i>Pna2</i> ₁	<i>Pna2</i> ₁	<i>Pnam</i>	<i>P2</i> ₁ / <i>c</i>	<i>P1</i>
cryst dimens (mm)	0.36 × 0.24 × 0.12	0.2 × 0.5 × 0.5	0.38 × 0.26 × 0.24	0.5 × 0.4 × 0.3	0.35 × 0.30 × 0.30	0.38 × 0.24 × 0.06
abs coeff (mm ⁻¹)	4.899	6.700	6.555	3.31	4.655	4.336
transmission factors	0.978, 0.602	0.119, 0.053	0.813, 0.644	0.309, 0.196	0.840, 0.613	1.000, 0.659
abs cor	ψ scans	ψ scans	ψ scans	ψ scans	ψ scans	ψ scans
diffractometer	Siemens P4	Siemens Stoe AED2	Siemens P4	Siemens Stoe AED2	Enraf-Nonius CAD4	Siemens P4
2θ range for data collection (deg)	4–48	4–47	4–51	4–50	4–50	4–40
no. of rflns collected	6840	4082	5303	4748	6342	4038
no. of indep rflns	6496 (<i>R</i> (int) = 0.0301)	3738 (<i>R</i> (int) = 0)	4093 (<i>R</i> (int) = 0.0526)	4408 (<i>R</i> (int) = 0)	6139 (<i>R</i> (int) = 0.0218)	3357 (<i>R</i> (int) = 0.0894)
refinement method	full-matrix least squares on <i>F</i> ²	full-matrix least squares on <i>F</i> ²	full-matrix least squares on <i>F</i> ²	full-matrix least squares on <i>F</i> ²	full-matrix least squares on <i>F</i> ²	full-matrix least squares on <i>F</i> ²
goodness of fit on <i>F</i> ²	1.078	0.7429	1.018	1.166	1.062	1.022
final <i>R</i> indices (<i>I</i> > 2σ(<i>I</i>))	<i>R</i> 1 = 0.0645, w <i>R</i> 2 = 0.1599	<i>R</i> 1 = 0.0473, <i>R</i> _w = 0.0633	<i>R</i> 1 = 0.0394, w <i>R</i> 2 = 0.0655	<i>R</i> 1 = 0.0698, w <i>R</i> 2 = 0.1893	<i>R</i> 1 = 0.0268, w <i>R</i> 2 = 0.0560	<i>R</i> 1 = 0.0436, w <i>R</i> 2 = 0.1127
<i>R</i> indices (all data)	<i>R</i> 1 = 0.1073, w <i>R</i> 2 = 0.1893		<i>R</i> 1 = 0.0639, w <i>R</i> 2 = 0.0743	<i>R</i> 1 = 0.0883, w <i>R</i> 2 = 0.2061	<i>R</i> 1 = 0.0371, w <i>R</i> 2 = 0.0598	<i>R</i> 1 = 0.0558, w <i>R</i> 2 = 0.1203

^a *R*1 = Σ(|*F*_o| - |*F*_c|)/Σ|*F*_o|. w*R*2 = [Σw(*F*_o² - *F*_c²)²/Σw(*F*_o²)²]^{1/2}. *R*_w = [Σw(|*F*_o| - |*F*_c|)²/Σw(|*F*_o|)²]^{1/2}. Goodness of fit = [Σw(*F*_o² - *F*_c²)²/(*n*_{obs} - *n*_{param})]^{1/2}. *w* = [σ²(*F*_o) + (*g*₁*P*)² + *g*₂*P*]⁻¹; *P* = [max(*F*_o²; 0) + 2*F*_c²]/3.

Table 3. Selected Bond Lengths (Å) and Angles (deg) for Complexes **5c**, **7a,c**, **8a**, **9b**, and **12a**^a

Complex 5c											
Pt(1)–C(7)	1.92(2)	Pt(1)–C(13)	2.00(2)	Pt(1)–C(19)	2.29(2)	Rh(1)–cent(Cp*)	1.873(17)	Rh(1)–C(13,14)	2.249(15)	C(13)–C(14)	1.25(2)
Pt(1)–C(18,19)	2.255(15)	Pt(1)–C(18)	2.379(14)	Rh(1)–C(18)	1.96(2)	C(18)–C(19)	1.21(2)	Pt(1)···Rh(1)	3.554(1)		
Rh(1)–C(13)	2.374(14)	Rh(1)–C(14)	2.29(2)	Rh(1)–P(1)	2.302(4)						
C(7)–Pt(1)–C(13)	86.8(6)	C(7)–Pt(1)–C(1)	88.5(6)	C(18)–Rh(1)–C(13,14)	82.3(6)	cent(Cp*)–Rh(1)–C(18)	119.7(7)				
C(1)–Pt(1)–C(19)	88.7(6)	C(13)–Pt(1)–C(18)	67.5(6)	cent(Cp*)–Rh(1)–C(13,14)	127.1(6)	cent(Cp*)–Rh(1)–P(1)	131.2(5)				
C(1)–Pt(1)–C(18,19)	103.2(6)	C(13)–Pt(1)–C(18,19)	81.5(6)	C(14)–C(13)–Pt(1)	178.9(13)	Pt(1)–C(13)–Rh(1)	108.4(7)				
C(14)–Rh(1)–P(1)	89.1(4)	C(18)–Rh(1)–P(1)	87.2(4)	C(13)–C(14)–Si(1)	141.7(13)	C(19)–C(18)–Rh(1)	176.4(14)				
C(18)–Rh(1)–C(13)	68.1(6)	P(1)–Rh(1)–C(13,14)	93.9(4)	Rh(1)–C(18)–Pt(1)	109.6(6)	C(18)–C(19)–Si(2)	151.2(13)				
Complex 7a											
Pt(1)–C(13)	2.41(2)	Pt(1)–C(14)	2.38(2)	Pt(1)–C(21)	2.46(2)	Pt(1)–C(13,14)	2.312(5)	Pt(1)–C(21,22)	2.31(5)	Ir(1)–cent(Cp*)	1.88(3)
Pt(1)–C(22)	2.30(2)	C(13)–C(14)	1.21(3)	C(21)–C(22)	1.21(3)	Ir(1)···Pt(1)	3.506(1)				
P(1)–Ir(1)–C(13)	86.3(6)	P(1)–Ir(1)–C(21)	87.7(6)	Ir(1)–C(21)–C(22)	160.9(18)	C(21)–C(22)–C(23)	154.2(21)				
C(13)–Ir(1)–C(21)	79.9(8)	C(1)–Pt(1)–C(7)	88.3(9)	C(1)–Pt(1)–C(13,14)	92.2(17)	C(7)–Pt(1)–C(21,22)	92.7(16)				
Ir(1)–C(13)–Pt(1)	106.0(9)	Ir(1)–C(13)–C(14)	176.9(17)	C(13,14)–Pt(1)–C(21,22)	86.8(11)	C(13)–Ir(1)–cent(Cp*)	128.4(13)				
C(13)–C(14)–C(15)	156.8(22)	Ir(1)–C(21)–Pt(1)	103.3(8)	C(21)–Ir(1)–cent(Cp*)	126.6(12)	P(1)–Ir(1)–cent(Cp*)	131.4(8)				
Complex 7c											
Pt(1)–C(1)	2.037(13)	Pt(1)–C(7)	2.037(13)	Pt(1)–C(19)	2.324(14)	Ir(1)–C(18)	1.98(2)	Ir(1)–P(1)	2.297(4)	Ir(1)–cent(Cp*)	1.886(1)
Pt(1)–C(14)	2.38(2)	Pt(1)–C(13)	2.442(13)	Pt(1)–C(18)	2.47(2)	C(13)–C(14)	1.25(2)	C(18)–C(19)	1.25(2)	Ir(1)···Pt(1)	3.5624(9)
Pt(1)–C(13,14)	2.31(1)	Pt(1)–C(18,19)	2.316(1)	Ir(1)–C(13)	1.981(13)						
C(1)–Pt(1)–C(7)	82.3(5)	C(1)–Pt(1)–C(19)	82.6(6)	Ir(1)–C(13)–Pt(1)	106.8(5)	C(13)–C(14)–Si(1)	142.4(13)				
C(7)–Pt(1)–C(14)	82.9(5)	C(7)–Pt(1)–C(13,14)	96.2(5)	C(19)–C(18)–Ir(1)	172.6(13)	C(18)–C(19)–Si(2)	145.9(13)				
C(1)–Pt(1)–C(18,19)	94.6(5)	C(13,14)–Pt(1)–C(18,19)	86.6(5)	cent(Cp*)–Ir(1)–C(13)	125.0(4)	cent(Cp*)–Ir(1)–C(18)	127.9(4)				
C(13)–Ir(1)–C(18)	76.9(6)	C(13)–Ir(1)–P(1)	90.1(4)	cent(Cp*)–Ir(1)–P(1)	130.2(1)						
C(18)–Ir(1)–P(1)	90.5(4)	C(14)–C(13)–Ir(1)	176.5(12)								
Complex 8a ^a											
Ir(1)–C(7)	1.990(13)	Ir(1)–P(1)	2.283(5)	Pd(1)–C(1)	1.994(13)	Ir(1)–cent(Cp*)	1.895(1)	Ir(1)···Pd(1)	3.435(1)	C(7)–C(8)	1.18(2)
Pd(1)–C(7)	2.383(12)	Pd(1)–C(8)	2.458(14)	Pd(1)–C(7,8)	2.348(1)						
C(7)–Ir(1)–C(7a)	81.0(7)	C(7)–Ir(1)–P(1)	88.7(4)	C(7)–C(8)–C(9)	159(2)	C(1)–Pd(1)–C(7,8)	92.29(2)				
C(1)–Pd(1)–C(1a)	82.8(7)	C(8)–C(7)–Ir(1)	177.2(12)	C(7,8)–Pd(1)–C(7a,8a)	92.62(2)	C(7)–Ir(1)–cent(Cp*)	126.38(3)				
Ir(1)–C(7)–Pd(1)	103.1(5)	C(7)–C(8)–C(9)	154(2)	P(1)–Ir(1)–cent(Cp*)	130.42(2)						
Complex 9b											
Pt–C(7)	1.995(5)	Pt–C(1)	2.002(4)	Pt–C(13)	2.307(4)	Rh–P	2.3034(14)	Rh–Cl	2.435(1)	C(13)–C(14)	1.218(6)
Pt–C(14)	2.345(4)	Pt–Cl	2.429(2)	Rh–C(13)	2.029(4)	Pt–C(13,14)	2.429(5)	Rh–cent(Cp*)	1.843(5)	Rh···Pt	3.371(1)
C(7)–Pt–C(1)	85.7(2)	C(7)–Pt–C(14)	88.5(2)	Pt–Cl–Rh	87.73(4)	C(14)–C(13)–Rh	173.0(4)				
C(7)–Pt–Cl	171.33(13)	C(1)–Pt–Cl	86.01(13)	Rh–C(13)–Pt	101.9(2)	C(13)–C(14)–C(15)	158.1(5)				
C(13)–Pt–Cl	75.65(12)	C(7)–Pt–C(13,14)	100.4(2)	P–Rh–cent(Cp*)	129.9(6)	Cl–Rh–cent(Cp*)	124.3(6)				
Cl–Pt–C(13,14)	87.9(2)	C(13)–Rh–P	90.23(13)	C(13)–Rh–cent(Cp*)	127.8(7)						
C(13)–Rh–Cl	80.67(12)	P–Rh–Cl	88.89(5)								
Complex 12a											
Ir(1)–C(1)	2.025(13)	Ir(1)–P(1)	2.299(3)	Ir(1)–Cl(1)	2.445(3)	Pd(1)–C(1)	2.341(10)	Pd(1)–Cl(1)	2.455(3)	Pd(1)–C(2)	2.457(10)
Ir(1)–cent(Cp*)	1.856(13)	Pd(1)–C(15)	1.993(11)	Pd(1)–C(9)	2.001(10)	Pd(1)–C(1,2)	2.325(10)	C(1)–C(2)	1.19(2)	Ir(1)···Pd(1)	3.362(1)
C(1)–Ir(1)–P(1)	88.6(3)	C(1)–Ir(1)–Cl(1)	84.4(3)	C(1)–Pd(1)–Cl(1)	78.0(3)	C(15)–Pd(1)–C(2)	83.2(4)				
P(1)–Ir(1)–Cl(1)	89.13(10)	cent(Cp*)–Ir(1)–Cl(1)	123.1(4)	Cl(1)–Pd(1)–C(1,2)	91.6(3)	C(15)–Pd(1)–C(1,2)	96.0(4)				
cent(Cp*)–Ir(1)–P(1)	132.4(4)	cent(Cp*)–Ir(1)–C(1)	125.0(6)	Ir(1)–Cl(1)–Pd(1)	86.65(9)	Ir(1)–C(1)–Pd(1)	100.4(5)				
C(15)–Pd(1)–C(9)	84.6(4)	C(9)–Pd(1)–Cl(1)	87.8(3)	C(2)–C(1)–Ir(1)	175.6(10)	C(1)–C(2)–C(3)	167.4(11)				

^a Symmetry transformation used to generate equivalent primed atoms: $x, y, -z + 1/2$.

more than 123° (124.3(6)–129.9(6)° in **9b**; 123.1(4)–132.4(4)° in **12a**). This structural fact, which is also apparent in the homobridged **5c**, **7a,c**, and **8a** compounds, has been previously observed in other mono- or dimetallic rhodium or iridium cyclopentadienyl systems.^{16b,24d,f} In both complexes, the metal–carbon distances $M(d^6)$ –C(centroid of ring) and $M'(d^8)$ –*ipso*–C(C₆F₅), respectively (see Table 3), and the $M(d^6)$ –P bond lengths are unexceptional. The structural parameters associated with the $M(\mu\text{-Cl})M'$ unit are comparable in both complexes; the bridging chloride is nearly symmetrically bonded to both metal centers with M –Cl distances (2.429(2), 2.435(1) Å, **9b**; 2.445(3), 2.455(3) Å, **12a**) and angles at chlorine (87.73(4)°, **9b**; 86.65(9)°, **12a**) comparable to related distances and angles found in doubly chloride bridged d^6 or d^8 homodimetallic compounds.^{24f,25} The alkynyl ligand bridges in the more commonly observed σ, π mode in which the α -C atom is σ -bound to rhodium (Rh–C(13) = 2.029(4) Å, **9b**) or

iridium (Ir(1)–C(1) = 2.025(13) Å, **12a**) and the unsaturated $C\equiv C$ bond is asymmetrically η^2 -bonded to Pt (**9b**) or Pd (**12a**) with the M –C $_{\alpha}$ distances (Pt–C(13) = 2.307(4) Å, Pd–C(1) = 2.341(10) Å) being slightly shorter than the corresponding M –C $_{\beta}$ (Pt–C(14) = 2.345(4) Å, Pd–C(2) = 2.457(10) Å) distances. The bend-back observed angles at C $_{\alpha}$ and C $_{\beta}$ (C $_{\alpha}$ /C $_{\beta}$: 173.0(4)/158.1(5)°, **9b**; 175.6(10)/167.4(11)°, **12a**) and $C\equiv C$ bond distances (1.218(6) Å, **9b**; 1.19(2) Å, **12a**) are similar to those observed for the related systems [(PPh₃)₂Pt(μ -H)-(μ - σ : η^2 C \equiv CPh)RhCp*(PMe₃)]²⁺ (**16a**; 173.9(9)/171(1)°, 1.21(1) Å)^{26a} and *trans*-[Pt₂(μ -H)(μ - σ : η^2 C \equiv CPh)(C₆F₅)₂-

(25) (a) Kukushkin, V. Y.; Belski, V. K.; Konovalov, V. E.; Shifrina, R. R.; Moiseev, A. I.; Vlasova, R. A. *Inorg. Chim. Acta* **1991**, *183*, 57 and references therein. (b) Hartley, F. R. *The Chemistry of Platinum and Palladium*; Applied Science Publishers: London, 1973. (c) Churchill, M. R.; Julis, S. A. *Inorg. Chem.* **1977**, *16*, 1488. (d) Elder, R. C.; Cruea, R. D.; Morrison, R. F. *Inorg. Chem.* **1976**, *15*, 1623. (e) Clark, H. C.; Ferguson, G.; Jain, V. K.; Parvez, M. *Inorg. Chem.* **1985**, *24*, 1477. (f) Churchill, M. R.; Julis, S. A.; Rotella, F. J. *Inorg. Chem.* **1977**, *16*, 1137.

(PPh₃)₂] (~163°, 1.23(2) Å).²⁷ The distortion of the alkyne fragment is significantly less pronounced than that reported recently in the alkynyl–chloride-bridged [Cp₂Zr(μ-Cl)(μ-C≡CCH₃)ZrCp₂] (168.2(3)/141.2(3)°, 1.286(4) Å).²⁸ The central M–Cl–C_α–C_β–M' cores are not planar. In both compounds, the M'(C₆F₅)₂ unit is directed toward the same side as the Cp* ring, and the dihedral angle between the M–Cl–C_α plane and the d⁸ (Pt or Pd) metal coordination plane (M'–Cl–*ipso*-C(C₆F₅) atoms and midpoint of C_α–C_β) is 43.5° in **9b** and 36.3° in **12a**. This puckering does not, however, cause any bonding between the metal centers (M···M' = 3.371(1) Å (**9b**), 3.362(1) Å (**12a**)).

In **5c** (Figure 3) the double-alkynyl bridging system displays an unsymmetrical σ/π disposition (type **IIb**, Chart 1) with both alkynyl ligands σ-bonded to different metals and η²-bonded on π-coordination to the other metal. This structural disposition has been previously found in several early (d¹–d¹)^{7b,8c,e,h,11a,29} and late (d⁸–d⁸)^{11b,c,13b} homodimetallic systems but only in a few heterodimetallic compounds: [Cp₂M(μ-σ:η²-C≡CR)(μ-η²:σ-C≡CR)M'Cp₂],^{8b} [Cp₂M(μ-σ:η²-C≡CSiMe₃)(μ-η²:σ-C≡CSiMe₃)Ni(PPh₃)] (M = Ti, Zr),^{8d} and [Cp₂Ti(μ-C≡C^tBu)₂Pt(PPh₃)].^{11d} The latter complexes are formally M(III)/M'(I) (M = Ti, Zr; M' = Ni, Pt) species and exhibit very short M–M' distances (2.728(1)–2.830(1) Å). In **5c** the Rh···Pt separation (3.554(1) Å) is considerably longer than that found in the hydride–alkynyl derivative **16a** (2.8265(8) Å)^{26a} or the separation found in the A-frame cation [ClPt(μ-σ:η²-C≡CMe)(μ-dppm)₂RhCO]⁺ (3.066(2), 3.086(2) Å),^{24b} ruling out any significant metal–metal interaction. Complex **5c** can hence be formally considered as the neutral zwitterionic Rh(III)/Pt(II) derivative [(PET₃)Cp*⁺Rh(μ-σ:η²-C≡CSiMe₃)(μ-η²:σ-C≡CSiMe₃)Pt⁻(C₆F₅)₂]. Significantly, there is little or no influence of the metal centers on the M–C bond lengths of the central RhPtC₄ framework. Thus, both the M–C σ-bonds (2.00(2), 1.96(2) Å) and the complexed η²-bond distances (2.379(14), 2.29(2) Å for Pt and 2.374(14), 2.29(2) Å for Rh) are identical, within experimental error, and are in the range usually found for these bonds.^{11b–d,13b,c,15b,d,g,22,24b,26,30} Both alkynyl fragments are only slightly bent at the inner C_α atoms (178.9(13), 176.4(14)°), while they deviate significantly from 180° at the outer atoms (141.7(13), 151.2(13)°). Again the central dimetallacycle core is not planar and the dihedral angle between the two planes defined by Rh(1)–C(18)–M(1) (M(1) midpoint C(13)–C(14)) and Pt(1)–C(1)–C(7)–C(13)–M(2) (M₂ midpoint C(18)–C(19)) is 28.7(5)°.

In contrast, as is shown in Figures 4–6, the structures of the mixed iridium compounds **7a**,¹⁴ **7c** (Ir–Pt), and **8a** (Ir–Pd) reveal that all these complexes possess a

chelating type structure (V-shape, **IIIb**; Chart 1). For complex **8a**, although disorder within crystallization solvent molecules and on one phenyl group (C(9)–C(14)) limited the accuracy of the determination, the presence of a connectivity similar to that found for **7a** and **7c** (Figures 4 and 5) is reflected in the view given in Figure 6.

In all complexes, the chelated metal center (Pt, **7a**, **7c**; Pd, **8a**) is located outside (1.0321(7) Å, **7a**; 1.0124(7) Å, **7c**; 0.8383(4) Å, **8a**) the corresponding starting 3-irida-1,4-diyne plane Ir(C≡C)₂. As in complexes **9b** and **12a**, in all of the cases the conformer found is that which places the Pt(C₆F₅)₂ unit on the same side as the Cp* ring. The resulting dihedral angles between the fragment IrC_αC_β plane and the corresponding platinum (**7a,c**) or Pd (**8a**) coordination planes are 38.3(6)° for **7a**, 37.1(4)° for **7c**, and 31.7(4)° for **8a**. The M'(d⁸)–C(η²) alkyne distances in **7c** and **8a** (2.31(4)–2.47(2) Å) are similar to those previously observed for **7a** (2.30(2)–2.46(2) Å). The structural parameters of the Ir–C≡C–E (E = C, Si) entities (see Table 3) are similar to those observed for related systems.^{12d,e,13b–e,14} In these complexes, the most remarkable feature is that the resulting bite angle C_α–Ir–C_β (79.9(8)°, **7a**; 76.9(6)°, **7c**; 81.0(7)°, **8a**) is notably smaller than those observed in related tweezer-like titanocene dinuclear derivatives {[L₂Ti(C≡CR)₂]ML_n} (L = η⁵-C₅H₄SiMe₃) studied (87.4(2)–102.8(2)°)^{2c,12e} and have a greater similarity to those found in dinuclear chelating type double-alkynyl-bridged complexes (V-shape, **IIIb**; Chart 1) formed with square-planar 3-platina-1,4-diyne species as building blocks:^{12d,13b–d} e.g. {[L₂Pt(μ-σ:η²-C≡CPh)₂]Pt(C₆F₅)₂} (L = 1/2 dppe, 79.3(4)°^{13b}). The Ir···M' nonbonded distances (3.506(1) Å in **7a**, 3.5624(9) Å in **7c**, and 3.435(1) Å in **8a**) are comparable to the Ir–Pt separation reported in the doubly chloride bridged cation [(PMe₃)Cp*Ir(μ-Cl)₂-Pt(dppp)]²⁺ (3.638 Å).^{24f}

Discussion

While cyclopentadienyl rings are typical metal auxiliaries widely used for the stabilization of alkynyl or related (vinylidenes, allenylidenes, etc.) groups in ruthenium(II) or iron(II) chemistry,^{3b,31} reported examples on Rh(III) and Ir(III) are extremely rare.^{16,17} The present study has shown that not only mono(alkynyl) cyclopentadienyl [Cp*M(C≡CR)X(PET₃)] (M = Rh (**1**), Ir (**2**)) but also bis(σ-alkynyl) [Cp*M(C≡CR)₂(PET₃)] (M

(26) (a) Cao, D. H.; Stang, P. J.; Arif, A. M. *Organometallics* **1995**, *14*, 2733. (b) Stang, P. J.; Cao, D. *Organometallics* **1993**, *12*, 996.

(27) Ara, I.; Falvello, L.; Fornies, J.; Martin, A.; Martinez, F.; Lalinde, E.; Moreno, M. T. *Organometallics* **1997**, *16*, 5392.

(28) Takahashi, T.; Nishihara, Y.; Sun, W.-H.; Fischer, R.; Nakajima, K. *Organometallics* **1997**, *16*, 2216.

(29) (a) Wood, G. L.; Knobler, C. B.; Hawthorne, M. F. *Inorg. Chem.* **1989**, *28*, 382. (b) Metzler, N.; Nöth, H. *J. Organomet. Chem.* **1993**, *454*, C5. (c) Erker, G.; Frömberg, W.; Mynott, R.; Gabor, B.; Krüger, C. *Angew. Chem., Int. Ed. Engl.* **1986**, *25*, 463.

(30) (a) Antwi-Nsiah, F. H.; Oke, O.; Cowie, M. *Organometallics* **1996**, *15*, 506. (b) Esteruelas, M. A.; Lahuerta, O.; Modrego, J.; Nürberg, O.; Oro, L. A.; Rodríguez, L.; Sola, E.; Werner, H. *Organometallics* **1993**, *12*, 266. (c) Osakada, K.; Matsumoto, K.; Yamamoto, T.; Yamamoto, A. *Organometallics* **1985**, *4*, 857.

(31) (a) *Comprehensive Organometallic Chemistry II*; Shriver, D. F., Bruce, M. I., Eds.; Wilkinson, G., Stone, F. G. A., Abel, E. W., Eds.; Elsevier: Oxford, U.K., 1995; Vol. 7. For recent work see: (b) Yi, C. S.; Liu, N.; Rheingold, A. L.; Liable-Sands, L. M.; Guzei, I. A. *Organometallics* **1997**, *16*, 3729. (c) de los Rios, I.; Jiménez-Tenorio, M.; Puerta, M. C.; Valerga, P. *J. Am. Chem. Soc.* **1997**, *119*, 6529. (d) Akita, M.; Kato, S.-I.; Terada, M.; Masaki, Y.; Tanaka, M.; Moro-Oka, Y. *Organometallics* **1997**, *16*, 2392. (e) Whittall, I. R.; Humphrey, M. G. *Organometallics* **1996**, *15*, 1935. (f) Coat, F.; Lapinte, C. *Organometallics* **1996**, *15*, 478. (g) Jia, G.; Xia, H. P.; Wu, W. F.; Ng, W. S. *Organometallics* **1996**, *15*, 3634. (h) Bruce, M. I.; Hall, B. C.; Zaitseva, N. N.; Skelton, B. W.; White, A. H. *J. Organomet. Chem.* **1996**, *522*, 307. (i) Peron, D.; Romero, A.; Dixneuf, P. H. *Organometallics* **1995**, *14*, 3319. (j) Nombel, P.; Lugan, N.; Mathieu, R. *J. Organomet. Chem.* **1995**, *503*, C22. (k) Sato, M.; Hayashi, Y.; Kumakura, S.; Shimizu, N.; Katada, M.; Kawata, S. *Organometallics* **1996**, *15*, 721. (l) Whittall, I. R.; Humphrey, M. G.; Hockless, D. C. R.; Skelton, B. W.; White, A. H. *Organometallics* **1995**, *14*, 3970. (m) Lang, H.; Blau, S.; Rheinwald, G. *J. Organomet. Chem.* **1995**, *492*, 81. (n) Ting, P.-C.; Lin, Y.-C.; Lee, G.-H.; Cheng, M.-C.; Wang, Y. *J. Am. Chem. Soc.* **1996**, *118*, 6433. (o) Lichtenberger, D. L.; Renshaw, S. K.; Bullock, R. M. *J. Am. Chem. Soc.* **1993**, *115*, 3276.

= Rh (**3**), Ir (**4**) derivatives of Rh(III) and Ir(III) are accessible. Complexes **1** and **2** increase the very small list of the mono(alkynyl) cyclopentadienyl rhodium(III) and iridium(III) derivatives presently known.^{15,16,17} Compounds **3** and **4** are very unusual. As far as we know, they are the first reported examples in which a Cp*ML (M = Rh, Ir) fragment is stabilized by two σ -alkynyl ligands. In particular, Maitlis et al. reported in 1982 that the preparation of complexes [Rh(C₅-Me₅)(C₄Ph₂HCPH=C₅Ph₂H₂)] (**13**) and [Rh(C₅Me₅)(C₈-Ph₄H₂)] (**14**) could be carried out via bis(alkynyl) intermediate species such as [Cp*Rh(C≡CPh)₂(NCMe)] and [Cp*Rh(C≡CPh)₂(HC≡CPh)];¹⁸ more recently, related neutral species [Cp*Rh(C≡CR)₂(α -alanine)] (R = Ph, tol) have been also suggested by Carmona et al.^{16b} in the course of the trimerization process that affords [Cp*Rh(η^4 -C₄HR₂C≡CR)] (**15**) by treatment of [Cp*Rh-(L-alaninate)(Cl)] with HC≡CPh and NEt₃. In this context, the synthesis of complexes **3** provide a strong indication that such species could exist. The stability of these complexes containing two alkynyl ligands mutually cis is surprising, since C-C alkynyl coupling reactions on Rh(III) to butadiynes have been observed previously.³²

Heterobridged mixed dinuclear neutral complexes [(PEt₃)Cp*M(μ -C≡CR)(μ -X)M'(C₆F₅)₂] (Rh, Ir-Pt, Pd, **9-12**) have been synthesized using mono(σ -alkynyl) complexes **1** and **2** as precursors. Several μ -Cl- μ -alkynyl-bridged homodinuclear (Zr-Zr)^{11a,28} and heterodinuclear (Ti-Cu,³³ Zr-Hf^{11a}) neutral compounds are known, and it should be mentioned that Stang has recently prepared, via an unusual C-H alkyne bond activation, two cationic heterodinuclear Rh-Pt (**16a**) and Ir-Pt (**16b**) derivatives [Cp*(PMe₃)M(μ -H)(μ - η^2 : σ -C≡CPh)Pt(PPh₃)₂](OTf)₂ containing a mixed μ -H- μ -C≡CR bridging system.²⁶ The X-ray crystal structure of complexes **9b** (Rh-Pt, C≡C^tBu) and **12a** (Ir-Pd, C≡CPh) revealed that the geometries at the metal centers and the σ -coordination of the alkynyl ligands to Rh or Ir have been preserved throughout the reaction, suggesting that the reactions of **1** and **2** with [cis-M'(C₆F₅)₂(thf)₂] (M' = Pt, Pd) complexes occur, via displacement of the thf ligands, by simple coordination of chloride and alkynyl (η^2 -side) groups to the Pd or Pt centers. At first sight this result is in contrast to the bonding characteristic found in the formal Rh(III)-Pt(II) cation [Cp*(PMe₃)Rh(μ -H)(μ - η^2 : σ -C≡CPh)Pt(PPh₃)₂]²⁺ (**16a**),^{26a} in which the phenylethynyl group is σ -bonded to Pt and η^2 -bonded to Rh, but clearly there are notable electronic and also steric differences on the organometallic fragments in **9-12** compared to **16**.

Different conclusions can be drawn from the structural data of some of the doubly alkynyl bridged complexes **5-8** formed by starting from **3** and **4** and [cis-M'(C₆F₅)₂(thf)₂]. The crystal structures of the heterodinuclear iridium derivatives **7a** (Ir-Pt, C≡CPh), **7c** (Ir-Pt, C≡CSiMe₃), and **8a** (Ir-Pd, C≡CPh) show that once again both alkynyl ligands remain σ -bonded to iridium, while the platinum (**7a,c**) and palladium (**8a**) centers are stabilized by η^2 -alkyne interactions, indicating that,

at least in these cases, the iridium center exhibits a stronger σ -alkynyl preference than the platinum or palladium. It is remarkable that complexes **7a,c** are also obtained using [cis-Pt(C₆F₅)₂(C≡CR)₂]²⁻ as unusual double alkynyl transfer reagents (Scheme 1). Monoalkynylation processes between transition-metal centers yielding dinuclear final compounds with one^{4n,34} or two^{11a,d,13b,c,29c} alkynyl ligands connecting the metal centers have been previously observed, but as far as we know, these are the first reported examples of double alkynylation. In contrast, the crystal structure of **5c** (Rh-Pt, C≡CSiMe₃) indicates that, in this system, the Pt atom seems to have a greater preference for the σ electronic density of the alkynyl groups than does the Rh center. This was of some surprise to us since, as mentioned in the Introduction, we had initially assumed that the alkynylation processes could be caused by the difference in the formal charge of the metal centers involved, but clearly this idea is not the determining factor since complex **5c** is obtained not only through the neutralization route but also by an unexpected σ -alkynyl ligand migration from Rh to Pt between the neutral mononuclear species **3c** and cis-Pt(C₆F₅)₂.

According to these results and on the basis of their spectroscopic data, particularly their IR spectra, while for the Rh-Pt complex **5a** we also favor a zwitterionic formulation with a σ/π double-alkynyl-bridged system, for **6a** (Rh-Pd) a chelating type is assumed. This latter formulation (**6a**) clearly shows that the preference for a σ -alkynyl bond should be higher in Pt than in Pd, and this reinforces other previous observations.^{13d,e} For instance, the preparation of (σ -alkynyl)platinum complexes by transmetalation of alkynyl groups using (σ -alkynyl)palladium complexes has been also recently reported.³⁵ It is reasonable to expect the greater σ -alkynyl preference of Ir and Pt over Rh and Pd and the easy alkynyl migration from Rh or Pd to Pt and from Pt to Ir on the basis of stronger M-C bonds with a third-row metal and greater kinetic lability of second-row metals.

There have been previous observations⁶⁻⁹ of the influence not only of the metal but also of the alkynyl substituents on the final structures of related double-alkynyl bridging systems. Changes in the alkynyl substituents also seem to have a pronounced effect on the systems reported here. In fact, all our attempts to prepare the corresponding heterometallic bis(μ -C≡C^t-Bu) derivatives have failed. However, the observation of σ/π -alkynide zwitterionic type structures for **5a** (Rh-Pt, Ph) and **5c** (Rh-Pt, SiMe₃) and chelating type structures for the related Ir-Pt derivatives **7a** (Ph) and **7c** (SiMe₃) clearly indicates that a change of R (Ph by SiMe₃) causes minor changes in the final disposition of the alkynyl ligands, which can be attributed principally to the influence of *electronic* effects of metal centers. This result is in contrast to previous observations on early-late [Cp₂Ti(C≡CR)₂ML_n] (M = Ni, Pt) heterodi-

(32) Bedford, R. B.; Hill, A. F.; Thompsett, A. R.; White, A. J. P.; Williams, D. J. *J. Chem. Soc., Chem. Commun.* **1996**, 1059.

(33) (a) Lang, H.; Frosch, W.; Wu, I. Y.; Blau, S.; Nuber, B. *Inorg. Chem.* **1996**, *35*, 6266. (b) Lang, H.; Blau, S.; Pritzkuw, H.; Zsolnai, L. *Organometallics* **1995**, *14*, 1850.

(34) (a) Berenguer, J. R.; Forniés, J.; Lalinde, E.; Martínez, F.; Urriolabeitia, E.; Welch, A. J. *J. Chem. Soc., Dalton Trans.* **1994**, 1291. (b) Ipaktschi, J.; Mirzaei, F.; Müller, B. G.; Beck, J.; Serafin, M. J. *Organomet. Chem.* **1996**, *526*, 363. (c) Akita, M.; Ishii, N.; Takabuchi, A.; Tanaka, M.; Moro-Oka, Y. *Organometallics* **1994**, *13*, 258. (d) Fritz, P. M.; Polborn, K.; Steinman, M.; Beck, W. *Chem. Ber.* **1989**, *122*, 889. (e) Bruce, M. I.; Abu-Salah, O. M.; Davis, P. E.; Raghavan, N. V. *J. Organomet. Chem.* **1974**, *64*, C48. (f) Lai, N.-S.; Tu, W.-C.; Peng, S.-M.; Lee, G.-H. *Organometallics* **1994**, *13*, 4652.

(35) Osakada, K.; Sakata, R.; Yamamoto, T. *Organometallics* **1997**, *16*, 5354.

metallic systems, which have essentially *flat* TiC_4M cores. In these planar dimers, the final tweezer-like or σ/π structures could be rationalized as the result of reducing steric congestion at the central core as a consequence of notable interactions between bulky ancillary ligands on Ni or Pt and alkyne substituents. Thus, whereas for bulky $\text{R} = \text{tBu}$ ($\text{ML}_n = \text{PtPPh}_3$)^{11d} or SiMe_3 ($\text{ML}_n = \text{NiPPh}_3$)^{8d} a σ/π bonding situation is formed, for $\text{R} = \text{SiMe}_3$ and $\text{ML}_n = \text{Ni}(\text{CO})$ ³⁶ or $[\text{Cp}_2\text{Ti}(\mu\text{-}\sigma\text{-}\eta^2\text{-C}\equiv\text{CPh})(\mu\text{-}\sigma\text{-}\eta^2\text{-C}\equiv\text{CSiMe}_3)\text{Ni}(\text{PPh}_3)]$ ^{8d} a tweezer-like structure is favored. In the d^6 – d^8 heterodimetallic systems presented here the dimers exhibit *nonplanar* structures which would seem to allow substantial control of steric factors.

Conclusion

In summary, mono- and bis(alkynyl) rhodium and iridium complexes **1–4** have been prepared from $[\text{Cp}^*\text{MX}_2(\text{PEt}_3)]$ ($\text{X} = \text{Cl}, \text{I}$) using classical metal–halogen exchange reactions with $\text{LiC}\equiv\text{CR}$ or $\text{AgC}\equiv\text{CR}$ and their reactivity toward $[\text{cis-}M'(\text{C}_6\text{F}_5)_2(\text{thf})_2]$ ($M' = \text{Pt}, \text{Pd}$) has been studied. Several hetero-bridged $\mu\text{-Cl-}\mu\text{-C}\equiv\text{CR}$ (**9–12**) and homobridged $(\mu\text{-C}\equiv\text{CR})_2$ (**5–8**) heterodinuclear Rh, Ir/Pt, Pd complexes have been synthesized, and interestingly, the final mixed platinum complexes **5a,c** and **7a,c** are obtained by starting from either terminal σ -alkynyl Rh and Ir or platinum precursors. The influence of the alkynyl substituents seems to be decisive on the final stability of the bis(μ -alkynide) heterometallic complexes, and only when the substituents are Ph or SiMe_3 are the final dimers easily formed. The reactions with *tert*-butylalkynyl groups lead to the formation of undefined products. X-ray diffraction and spectroscopic data on the final heterodinuclear products indicate that the observed metal site preference for σ coordination to alkynyl bridging ligands in these homobridged dimers follows the order $\text{Ir} > \text{Pt} > \text{Rh} > \text{Pd}$. These observations are consistent with the expected stronger M–C bonds with a third-row metal than with a second-row metal and with the greater kinetic lability of the second-row metals.

Experimental Section

All manipulations were carried out under a nitrogen atmosphere. Solvents (hexane, alkanes mixture) were dried by standard procedures and distilled under dry N_2 before use. Moist thf employed for quenching alkynylation reactions was RPE grade, used as received.

The instruments and procedures used have been previously reported.²² All coupling constants are given in Hz. Mass spectra were obtained in a VG Autospec double-focusing mass spectrometer operating in the FAB^+ mode, except for complex **11a'** (HP-5989B mass spectrometer using the $\text{ES}(-)$ technique).

$\text{Q}_2[\text{cis-Pt}(\text{C}_6\text{F}_5)_2(\text{C}\equiv\text{CR})_2]$ ($\text{Q} = \text{PMePh}_3$, $\text{R} = \text{Ph}$;^{21d} $\text{Q} = \text{NBu}_4$, $\text{R} = \text{tBu}$,^{21d} SiMe_3 ^{13d}), $[\text{cis-}M'(\text{C}_6\text{F}_5)_2(\text{thf})_2]$ ($M' = \text{Pd}, \text{Pt}$),³⁷ and AgClO_4 ³⁸ were prepared by published methods; $[\text{AgC}\equiv\text{CPh}]_n$ ³⁹ was prepared by treating an aqueous ammoniacal solution of AgNO_3 with $\text{HC}\equiv\text{CPh}$.

(36) Lang, H.; Imhof, W. *Chem. Ber.* **1992**, *125*, 1307.

(37) Usón, R.; Forniés, J.; Tomás, M.; Menjón, B. *Organometallics* **1985**, *4*, 1912.

(38) Smith, G. F.; Ring, F. *J. Am. Chem. Soc.* **1937**, *59*, 1889.

(39) van Koten, G.; Noltes, J. G. In *Comprehensive Organometallic Chemistry*; Wilkinson, G.; Stone, F. G. A.; Abel, E. W., Eds.; Pergamon Press: Oxford, U.K., 1982; Vol. 2, p 721.

$[\text{Cp}^*\text{MCl}_2(\text{PEt}_3)]$ ($\text{M} = \text{Rh}, \text{Ir}$) were prepared by a procedure similar to that previously described for related derivatives by Maitlis *et al.*¹⁹ $[\text{Cp}^*\text{IrI}_2(\text{PEt}_3)]$ was prepared from $[\text{Cp}^*\text{IrCl}_2(\text{PEt}_3)]$ and excess NaI in acetone.

Data for $[\text{Cp}^*\text{RhCl}_2(\text{PEt}_3)]$: Anal. Calcd for $\text{C}_{16}\text{H}_{30}\text{Cl}_2\text{PRh}$: C, 44.95; H, 7.07. Found: C, 44.89; H, 6.90. MS: m/z 426 $[\text{M}]^+$ 8%; 391 $[\text{M} - \text{Cl}]^+$ 100%. ¹H NMR (CDCl_3 , δ): at 15 °C, 2.06 (m, PCH_2CH_3 , 6H); 1.64 (d, ⁴ $J_{\text{P-H}}$ 3.01, Cp^* , 15 H); 1.13 (dt, ³ $J_{\text{P-H}}$ 15.2, ³ $J_{\text{H-H}}$ 7.6, $\text{P-CH}_2\text{-CH}_3$, 9H). ¹³C NMR (CDCl_3 , δ): at 15 °C, 99.11 (dd, ¹ $J_{\text{Rh-C}}$ 6.7, ² $J_{\text{P-C}}$ 2.9, C_5Me_5); 16.92 (d, ¹ $J_{\text{P-C}}$ 27.2, PCH_2CH_3); 9.38 (d, ² $J_{\text{Rh-C}}$ 1.3, $\text{C}_5(\text{CH}_3)_5$); 8.08 (d, ² $J_{\text{P-C}}$ 4.6, PCH_2CH_3). ³¹P NMR (CDCl_3 , δ): at 15 °C, 28.0 (d, ¹ $J_{\text{P-Rh}}$ 137.8).

Data for $[\text{Cp}^*\text{IrCl}_2(\text{PEt}_3)]$: Anal. Calcd for $\text{C}_{16}\text{H}_{30}\text{Cl}_2\text{IrP}$: C, 37.21; H, 5.85. Found: C, 36.73; H, 6.23. MS: m/z = 516 $[\text{M}]^+$ 27%; 481 $[\text{M} - \text{Cl}]^+$ 100%; 363 $[\text{IrCp}^*\text{Cl}]^+$ 30%. ¹H NMR (CDCl_3 , δ): at 15 °C, 2.10 (m, PCH_2CH_3 , 6H); 1.66 (d, ⁴ $J_{\text{P-H}}$ 1.7, Cp^* , 15 H); 1.1 (dt, ³ $J_{\text{P-H}}$ 15.5, ³ $J_{\text{H-H}}$ 7.7, PCH_2CH_3 , 9H). ¹³C NMR (CDCl_3 , δ): at 15 °C, 90.9 (d, ² $J_{\text{P-C}}$ 2.7, C_5Me_5); 15.77 (d, ¹ $J_{\text{P-C}}$ 34.1, PCH_2CH_3); 8.68 (s, $\text{C}_5(\text{CH}_3)_5$); 7.19 (d, ² $J_{\text{P-C}}$ 3.9, PCH_2CH_3). ³¹P NMR (CDCl_3 , δ): at 15 °C, -6.3 (s).

Data for $[\text{Cp}^*\text{IrI}_2(\text{PEt}_3)]$: Anal. Calcd for $\text{C}_{16}\text{H}_{30}\text{I}_2\text{IrP}$: C, 27.48; H, 4.32. Found: C, 27.66; H, 4.15. MS: m/z = 699 $[\text{M}]^+$ 5%; 573 $[\text{M} - \text{I}]^+$ 100%; 455 $[\text{IrCp}^*\text{I}]^+$ 27%. ¹H NMR (CDCl_3 , δ): at 15 °C, 2.26 (m, PCH_2CH_3 , 6H); 1.93 (d, ⁴ $J_{\text{P-H}}$ 1.6, Cp^* , 15 H); 1.12 (dt, ³ $J_{\text{P-H}}$ 15.2, ³ $J_{\text{H-H}}$ 7.7, PCH_2CH_3 , 9H). ¹³C NMR (CDCl_3 , δ): at 15 °C, 92.61 (d, ² $J_{\text{P-C}}$ 2.5, C_5Me_5); 21.41 (d, ¹ $J_{\text{P-C}}$ 35.94, PCH_2CH_3); 10.57 (d, ³ $J_{\text{P-C}}$ 0.8, $\text{C}_5(\text{CH}_3)_5$); 9.92 (d, ² $J_{\text{P-C}}$ 4.8, PCH_2CH_3). ³¹P NMR (CDCl_3 , δ): at 15 °C, -19.7 (s).

Reaction of $[\text{Cp}^*\text{RhCl}_2(\text{PEt}_3)]$ with $\text{LiC}\equiv\text{CPh}$ (Complex **1a).** $[\text{Cp}^*\text{RhCl}_2(\text{PEt}_3)]$ (0.3 g, 0.7 mmol) was added, at low temperature (-20 °C), to a freshly prepared solution of $\text{LiC}\equiv\text{CPh}$ (2.81 mmol, molar ratio $\text{Rh/Li} = 1/4$) in thf (20 mL), prepared from $\text{HC}\equiv\text{CPh}$ (0.32 mL, 2.81 mmol) and Li^nBu (1.75 mL, 2.81 mmol, hexane solution 1.6 M), and the mixture was stirred for ca. 2 min. The resulting red solution was rapidly hydrolyzed with moist thf (3 mL) and evaporated to dryness. The oily residue was treated with toluene/hexane (30 mL, 2/1) and filtered. Evaporation of the filtrate yielded an oily residue. The NMR data of this oil (~90% yield based on Rh) shows it to be $[\text{Cp}^*\text{Rh}(\text{C}\equiv\text{CPh})\text{Cl}(\text{PEt}_3)]$ (**1a**) along with small amounts of $[\text{Cp}^*\text{RhCl}_2(\text{PEt}_3)]$ (~12%) and $[\text{Cp}^*\text{Rh}(\text{C}\equiv\text{CPh})_2(\text{PEt}_3)]$ (**3a**; ~14%). As all attempts to purify **1a** were unsuccessful, this complex, **1a**, was spectroscopically characterized from this mixture.

Data for **1a**: MS: m/z = 457 $[\text{M} - \text{Cl}]^+$ 62%; 391 $[\text{M} - \text{C}_2\text{-Ph}]^+$ 36%; 372 $[\text{M} - (\text{PEt}_3) - 2\text{H}]^+$ 28%, 356 $[\text{Cp}^*\text{Rh}(\text{PEt}_3)]^+$ 79%, 237 $[\text{Cp}^*\text{Rh}]^+$ 91%. ¹H NMR (CDCl_3 , δ): at 15 °C, 7.29, 7.16, 7.05 (m, Ph, 5H); 2.04 (m, PCH_2CH_3 , 6H); 1.75 (d, ⁴ $J_{\text{P-H}}$ 2.6, Cp^* , 15 H); 1.16 (m, PCH_2CH_3 , 9H). ³¹P NMR (CDCl_3 , δ): at 15 °C, 32.9 (d, ¹ $J_{\text{P-Rh}}$ 131).

We have also attempted to synthesize **1a**, by treating $[\text{Cp}^*\text{RhCl}_2(\text{PEt}_3)]$ with an excess (1:3) of $[\text{AgC}\equiv\text{CPh}]_n$, but NMR (³¹P) only detected mixtures of **1a**, **3a**, and $[\text{Cp}^*\text{RhCl}_2(\text{PEt}_3)]$ with undefined products.

Preparation of $[\text{Cp}^*\text{Rh}(\text{C}\equiv\text{C}^t\text{Bu})\text{Cl}(\text{PEt}_3)]$ (1b**).** A solution of Li^nBu in hexane (1.6 N, 3.49 mL, 5.58 mmol) was added dropwise for 5 min to a thf solution (30 mL) of $\text{HC}\equiv\text{C}^t\text{Bu}$ (0.76 mL, 5.62 mmol) at -20 °C. After 20 min of stirring $[\text{Cp}^*\text{RhCl}_2(\text{PEt}_3)]$ (0.4 g, 0.94 mmol) was added and the mixture was stirred for 10 min. The resulting red solution was hydrolyzed with moist thf (3 mL) and evaporated to dryness. The oily residue was treated with toluene/hexane (30 mL, 1/1) and filtered. Evaporation of the filtrate and treatment of the final residue with cold hexane afforded **1b** as an orange solid. Yield 33%.

Data for **1b**: Anal. Calcd for $\text{C}_{22}\text{H}_{39}\text{ClPRh}$: C, 55.90; H, 8.3. Found: C, 56.00; H, 7.91. MS: m/z = 471 $[\text{M} + \text{H}]^+$ 7%; 437 $[\text{M} - \text{Cl}]^+$ 54%; 391 $[\text{M} - \text{C}_2^t\text{Bu}]^+$ 29%; 355 $[\text{M} - \text{Cl} - \text{C}_2^t\text{Bu}]^+$ 25%. ¹H NMR (CDCl_3 , δ): at 15 °C, 1.99 (m, PCH_2CH_3 , 6H); 1.68 (d, ⁴ $J_{\text{P-H}}$ 2.5, Cp^* , 15 H); 1.16 (s, ^tBu , 9H); 1.12 (m,

PCH₂CH₃, 9H). ¹³C NMR (CDCl₃, δ): at 15 °C, 111.35 (dd, ²J_{Rh-C} 9.14, ³J_{P-C} 2.32, C_β, -C≡CR); 98.85 (dd, ¹J_{Rh-C} 5.2, ²J_{P-C} 2.9, C₅Me₃); 82.7 (dd, ¹J_{Rh-C} 52.8, ²J_{P-C} 38.1, C_α, -C≡CR); 32.56 (d, ⁴J_{Rh-C} 0.63, -C(CH₃)₃, C≡CR); 28.83 (d, ³J_{Rh-C} 2.2, -CMe₃, C≡CR); 17.53 (d, ¹J_{P-C} 29.6, PCH₂CH₃); 9.20 (d, ²J_{Rh-C} 1.3, C₅(CH₃)₅); 8.0 (d, ²J_{P-C} 4.1, PCH₂CH₃). ³¹P NMR (CDCl₃, δ): at 15 °C, 32.6 (d, ¹J_{P-Rh} 133).

Preparation of a Mixture of [Cp*Rh(C≡CSiMe₃)Cl(PET₃)] (1c) and 3c. [Cp*RhCl₂(PET₃)] (0.4 g, 0.94 mmol) was added to a cold (-20 °C) solution of LiC≡CSiMe₃ (3.7 mmol) in thf (30 mL). The mixture was stirred for 2 min, hydrolyzed, and evaporated to dryness; the residue was then extracted with toluene/hexane (30 mL, 1/1) and the extracts were filtered. Evaporation of the filtrate under reduced pressure yielded an oily residue which was identified by NMR spectroscopy (³¹P and ¹H) as a mixture of complexes **1c** and **3c** in a 2:1 ratio. Complex **1c** was spectroscopically characterized from this mixture. Using a shorter reaction time, lower temperature, or less excess of LiC≡CSiMe₃ (1:1 or 1:2) mixtures of [Cp*RhCl₂(PET₃)] and **3c**, sometimes with **1c** also, were always obtained.

Data for **1c**: ¹H NMR (CDCl₃, δ): at 15 °C, 1.97 (m, PCH₂CH₃, 6H); 1.70 (d, ⁴J_{P-H} 2.5, Cp*, 15 H); 1.12 (m, PCH₂CH₃, 9H); 0.04 (s, SiMe₃, 9H). ¹³C NMR (CDCl₃, δ): at 15 °C, 126.9 (dd, ¹J_{Rh-C} 50.2, ²J_{P-C} 34.6, C_α, -C≡CR); 109.0 (dd, ²J_{Rh-C} 7.8, ³J_{P-C} 2.3, C_β, -C≡CR); 99.6 (dd, ¹J_{Rh-C} 5.1, ²J_{P-C} 2.8, C₅Me₃); 17.5 (d, ¹J_{P-C} 29.4, PCH₂CH₃); 9.28 (d, ²J_{Rh-C} 1.3, C₅(CH₃)₅); 7.93 (d, ²J_{P-C} 4.2, PCH₂CH₃); 1.17 (s, SiMe₃). ³¹P NMR (CDCl₃, δ): at 15 °C 32.6 (d, ¹J_{P-Rh} 132).

Preparation of [Cp*Ir(C≡CPh)Cl(PET₃)] (2a). A mixture of 0.25 g (0.48 mmol) of [Cp*IrCl₂(PET₃)] and [AgC≡CPh]_n (0.2 g, 0.96 mmol) in CH₂Cl₂ (30 mL) was stirred with exclusion of light and monitored by ³¹P NMR. After 1 h a 1:1 mixture of [Cp*IrCl₂(PET₃)] and **2a** is observed. After 4 h, the iridium dichloride had been converted into **2a**. Traces of **4a** and of a new unidentified species (δ -5.9) were also observed. The excess of [AgC≡CPh]_n and AgCl formed was then filtered and the resulting pale yellow solution evaporated to dryness. Addition of cold hexane (5 mL) to the residue afforded **2a** as a yellow solid. Yield: 45%.

Data for **2a**: Anal. Calcd for C₂₄H₃₅ClIrP: C, 49.50; H, 6.05. Found: C, 49.10; H, 6.38. MS: *m/z* = 582 [M]⁺ 66%; 547 [M - Cl]⁺ 100%; 481 [M - C₂Ph]⁺ 56%. ¹H NMR (CDCl₃, δ): at 15 °C, 7.24, 7.16, 7.03 (m, Ph, 5 H); 2.09 (m, PCH₂CH₃, 6H); 1.80 (d, ⁴J_{P-H} 1.4, Cp*, 15 H); 1.11 (m, PCH₂CH₃, 9H). ¹³C NMR (CDCl₃, δ): at 15 °C, 131.55 (s, *o*-C, Ph); 127.5 (s, *m*-C, Ph); 124.38 (s, Ph); 102.09 (s, C_β, -C≡CR); 93.73 (s, C₅Me₃); 16.8 (d, ¹J_{P-C} 35.5, PCH₂CH₃); 9.12 (s, C₅(CH₃)₅); 7.62 (d, ²J_{P-C} 3.8, PCH₂CH₃). ³¹P NMR (CDCl₃, δ): at 15 °C, -7.3 (s).

Reaction of [Cp*IrCl₂(PET₃)] with LiC≡CPh. [Cp*IrCl₂(PET₃)] (0.35 g, 0.678 mmol) was added at low temperature to a freshly prepared solution of LiC≡CPh in thf (molar ratio Ir:Li = 1:6), and the mixture was stirred at room temperature overnight. The resulting orange solution was evaporated to dryness and the residue extracted with toluene/hexane (1/9), and the extracts were filtered. Evaporation of the filtrate to dryness and treatment of the residue with hexane yielded a beige solid (0.2 g). NMR analyses of this solid revealed that it was an approximately equimolecular mixture of the mono- and bis(alkynyl) iridium derivatives **2a** and **4a**.

By using a lower excess of LiC≡CPh (Ir/LiC≡CPh 1/3) and a shorter reaction time (1 h), a pale orange solid (57% yield) was obtained and identified as [Cp*IrCl₂(PET₃)] with a small amount of **2a** (less than 10%).

The reaction of [Cp*IrCl₂(PET₃)] with a large excess of LiC≡CPh (Ir/LiC≡CPh 1/10) in thf was monitored by ³¹P NMR spectroscopy. After 1 h of reaction the dichloride precursor had not been yet consumed and a mixture of this and **2a** in a ca. 2:1 ratio, plus a small amount of **4a** (less than 5%), was clearly observed. After the mixture was stirred for 12 h, all the dichloride precursor reacted, giving an equimolecular

mixture of **2a** and **4a**. Small amounts of unidentified decomposition products (δ -11.99, -12.6, and -16.25) were also observed. Longer reaction times only produced an slight increase of the proportion of **4a**, 40:60 being the final ratio of **2a** to **4a** after 3 days.

Preparation of [Cp*Ir(C≡CPh)I(PET₃)] (2a'). An orange solution of [Cp*IrI₂(PET₃)] (0.15 g, 0.214 mmol) in CH₂Cl₂ (30 mL) was treated with an excess of [AgC≡CPh]_n (0.135 g, 0.64 mmol) and the mixture refluxed for 90 min. Control by ³¹P NMR of the reaction mixture showed the presence of **4a**, **2a'**, and the precursor [Cp*IrI₂(PET₃)] (ratio ca. 12:70:18). The mixture was refluxed for another 30 min and then filtered. Evaporation of the resulting pale orange solution and addition of 20 mL of diethyl ether gave **2a'** as an orange solid. Yield: 56%.

Data for **2a'**: Anal. Calcd for C₂₄H₃₅IIrP: C, 42.79; H, 5.24. Found: C, 42.56; H, 5.10. MS: *m/z* = 674 [M]⁺ 25%; 648 [Cp*Ir(C₂Ph)(PET₃)]⁺ 26%; 573 [M - C₂Ph]⁺ 55%, 547 [M - I]⁺ 100%. ¹H NMR (CDCl₃, δ): at 15 °C, 7.17, 7.00 (m, Ph, 5 H); 2.15 (m, PCH₂CH₃, 6H); 1.94 (s, Cp*, 15 H); 1.13 (m, PCH₂CH₃, 9H). ¹³C NMR (CDCl₃, δ): at 15 °C, 131.6 (s, *o*-C, Ph); 129.3 (s, *i*-C, Ph); 127.45 (s, *m*-C, Ph); 124.2 (s, *p*-C, Ph); 103.13 (s, C_β, -C≡CR); 94.14 (d, ²J_{P-C} 2.5, C₅Me₃); 19.32 (d, ¹J_{P-C} 36.4, PCH₂CH₃); 9.89 (s, C₅(CH₃)₅); 8.7 (d, ²J_{P-C} 4, PCH₂CH₃). ³¹P NMR (CDCl₃, δ): at 15 °C, -12.7 (s).

Preparation of [Cp*Ir(C≡CSiMe₃)I(PET₃)] (2c'). To a cooled (-20 °C) freshly prepared solution of LiC≡CSiMe₃ (6.43 mmol) in thf (30 mL) was added [Cp*IrI₂(PET₃)] (0.3 g, 0.43 mmol). The mixture was stirred for 50 min, hydrolyzed with moist thf (~3 mL), and evaporated to dryness. The oily residue was extracted with toluene/hexane (30 mL, 2/1), and the extracts were filtered. Evaporation of the filtrate yielded an orange oil, characterized as complex **2c'** by NMR spectroscopy (¹H and ³¹P). Yield: 94%.

Data for **2c'**: MS: *m/z* = 669 [M]⁺ 22%; 573 [M - C₂SiMe₃ + H]⁺ 100%, 543 [M - I + H]⁺ 75%; 455 [Cp*IrI + H]⁺ (98%). ¹H NMR (CDCl₃, δ): at 15 °C, 2.09 (m, PCH₂CH₃, 6H); 1.87 (d, ⁴J_{P-H} 1.6, Cp*, 15 H); 1.08 (m, PCH₂CH₃, 9H); 0.02 (s, SiMe₃, 9H). ¹³C NMR (CDCl₃, δ): at 15 °C, 105.32 (d, ³J_{P-C} 0.83, C_β, -C≡CR); 103.48 (d, ²J_{P-C} 21.31, C_α, C≡CPh); 94.10 (d, ²J_{P-C} 2.75, C₅Me₃); 19.39 (d, ¹J_{P-C} 36.48, PCH₂CH₃); 9.81 (d, ³J_{P-C} 0.88, C₅(CH₃)₅); 8.83 (d, ²J_{P-C} 4.2, PCH₂CH₃); 1.84 (s, SiMe₃). ³¹P NMR (CDCl₃, δ): at 15 °C, -13.2 (s).

Preparation of [Cp*Rh(C≡CR)₂(PET₃)] (R = Ph (3a), ^tBu (3b), SiMe₃ (3c)). A typical preparation for complex **3a** was as follows:

[Cp*RhCl₂(PET₃)] (0.4 g, 0.94 mmol) was added at low temperature (-20 °C) to a solution of LiC≡CPh (molar ratio Rh:Li = 1:5) in thf (20 mL), and the mixture was stirred for 30 min. The resulting red solution was evaporated to dryness, the resulting red solid was extracted with toluene/hexane (~100 mL, 2/1), and the extract was filtered and evaporated to dryness. Treatment of the solid residue with cold hexane afforded **3a** as a brown solid. Yield: 69%.

Data for **3a**: Anal. Calcd for C₃₂H₄₀PRh: C, 68.81; H, 7.21. Found: C, 68.61; H, 6.91. MS: *m/z* = 558 [M]⁺ 27%; 441 [M - (PET₃)]⁺ 17%; 356 [Cp*Rh(PET₃)]⁺ 100%. ¹H NMR (CDCl₃, δ): at 15 °C, 7.28, 7.16, 7.04 (m, Ph, 10H); 2.03 (m, PCH₂CH₃, 6H); 1.90 (d, ⁴J_{P-H} 2.27, Cp*, 15 H); 1.17 (dt, ³J_{P-H} 15.7, ³J_{H-H} 7.8, PCH₂CH₃, 9H). ¹³C NMR (CDCl₃, δ): at -50 °C, 130.9 (s, *o*-C, Ph); 129.0 (s, *i*-C, Ph); 127.5 (s, *m*-C, Ph); 124.0 (s, *p*-C, Ph); 103.7 (dd, ¹J_{Rh-C} 53, ²J_{P-C} 30.8, C_α, -C≡CR); 102.9 (dd, ²J_{Rh-C} 10.3, ³J_{P-C} 2.7, C_β, -C≡CR); 99.8 (dd, ¹J_{Rh-C} 3.7, ²J_{P-C} 2.8, C₅Me₃); 17.6 (d, ¹J_{P-C} 31, PCH₂CH₃); 9.8 (d, ²J_{Rh-C} 1, C₅(CH₃)₅); 7.9 (d, ²J_{P-C} 3.4, PCH₂CH₃). ³¹P NMR (CDCl₃, δ): at 15 °C, 37.2 (d, ¹J_{P-Rh} 122).

Complexes **3b** and **3c** were obtained similarly by starting from [Cp*RhCl₂(PET₃)] (0.4 g, 0.94 mmol) and LiC≡CR (R = ^tBu, 5.6 mmol, **3b**; R = SiMe₃, 6.18 mmol, **3c**). The reaction times were 75 min for **3b** and 30 min for **3c**. The final residues were extracted with 30 mL of a toluene/hexane (1/1) mixture

and the extracts filtered. The resulting filtrates were evaporated again, yielding **3b** as a gummy brown solid (47% yield) and **3c** as a red oil (87% yield), which were characterized by spectroscopic methods in solution.

Data for **3b**: Satisfactory analyses of this complex could not be obtained. Anal. Calcd for $C_{28}H_{48}PRh$: C, 64.85; H, 9.32. Found: C, 62.96; H, 7.63. MS: $m/z = 519 [M + H]^+$ 18%; 437 $[M - C_2C^*Bu]^+$ 12%; 401 $[M - (PEt_3)]^+$ 92%; 356 $[Cp^*Rh(PEt_3)]^+$ 100%. 1H NMR ($CDCl_3$, δ): at 15 °C, 1.90 (m, PCH_2CH_3 , 6H); 1.75 (d, $^4J_{P-H}$ 2.4, Cp^* , 15 H); 1.14 (s, 1Bu , 18H); 1.09 (m, PCH_2CH_3 , 9H). ^{13}C NMR ($CDCl_3$, δ): at -50 °C, 108.7 (dd, $^2J_{Rh-C}$ 9.7, $^3J_{P-C}$ 3, C_β , $-C\equiv CR$); 98.7 (t, $^1J_{Rh-C} \approx ^2J_{P-C}$ 3.5, C_5Me_5); 81.46 (dd, $^1J_{Rh-C}$ 53.9, $^2J_{P-C}$ 33.6, C_α , $-C\equiv CR$); 32.5 (s, $-C(CH_3)_3$, $C\equiv CR$); 28.9 (s, $-CMe_3$, $C\equiv CR$); 18.4 (d, $^1J_{P-C}$ 31.5, PCH_2CH_3); 9.6 (d, $^2J_{Rh-C}$ 1, $C_5(CH_3)_5$); 8.4 (d, $^2J_{P-C}$ 3, PCH_2CH_3). ^{31}P NMR ($CDCl_3$, δ): at 15 °C, 37.3 (d, $^1J_{P-Rh}$ 124).

Data for **3c**: MS: $m/z = 551 [M + H]^+$ 19%; 453 $[M - C_2SiMe_3]^+$ 14%; 433 $[M - (PEt_3) + H]^+$ 50%; 356 $[Cp^*Rh(PEt_3)]^+$ 100%. 1H NMR ($CDCl_3$, δ): at 15 °C, 1.93 (m, PCH_2CH_3 , 6H); 1.78 (d, $^4J_{P-H}$ 2.4, Cp^* , 15 H); 1.09 (dt, $^3J_{P-H}$ 16, $^3J_{H-H}$ 7.6, PCH_2CH_3 , 9H); 0.02 (s, $SiMe_3$, 18H). ^{13}C NMR ($CDCl_3$, δ): at -50 °C, 125.9 (dd, $^1J_{Rh-C}$ 49, $^2J_{P-C}$ 28, C_α , $-C\equiv CR$); 106.2 (dd, $^2J_{Rh-C}$ 8.4, $^3J_{P-C}$ 2.6, C_β , $-C\equiv CR$); 99.5 (t, $^1J_{Rh-C} \approx ^2J_{P-C}$ 3.1, C_5Me_5); 17.7 (d, $^1J_{P-C}$ 31, PCH_2CH_3); 9.6 (s, $C_5(CH_3)_5$); 7.9 (d, $^2J_{P-C}$ 3.3, PCH_2CH_3); 1.4 (s, $SiMe_3$, $C\equiv CR$). ^{31}P NMR ($CDCl_3$, δ): at 15 °C, 36.6 (d, $^1J_{P-Rh}$ 124).

Preparation of $[Cp^*Ir(C\equiv CPh)_2(PEt_3)]$ (4a**). Method A.** This complex was prepared by following a procedure similar to that for complexes **3** by treating $[Cp^*IrI_2(PEt_3)]$ (0.25 g, 0.36 mmol) with an excess of $LiC\equiv CPh$ (5.36 mmol, molar ratio 1:15). The reaction time was 6.5 h, the final residue was extracted with 30 mL of CH_2Cl_2 , and the extracts were filtered. The filtrate was evaporated to dryness, yielding **4a** as a beige solid. Yield: 90%. Control by ^{31}P NMR revealed the following ratios (%) for **4a**, **2a**, and $[Cp^*IrI_2(PEt_3)]$ during the course of the reaction: (i) at 40 min ~3:26:71; (ii) at 2 h, 21:54:25; (iii) at 5 h, 76:18:6; (iv) at 6 h, 92:8:-.

Method B. A mixture of 0.15 g (0.22 mmol) of $[Cp^*IrI_2(PEt_3)]$ and $[AgC\equiv CPh]_n$ (0.17 g, 0.84 mmol) in CH_2Cl_2 (30 mL) was stirred at room temperature protected from the light for 4 days. The excess of $[AgC\equiv CPh]_n$ and AgI formed was then filtered and the resulting pale yellow solution evaporated to dryness. Addition of cold hexane (5 mL) to the residue afforded **4a**. Yield: 78%.

Data for **4a**: Anal. Calcd for $C_{32}H_{40}IrP$: C, 59.33; H, 6.22. Found: C, 57.47; H, 5.58. The analyses do not fit well, probably due to small amounts of crystallized CH_2Cl_2 (**4a**·0.25 CH_2Cl_2 : C, 57.89; H, 6.10). MS: $m/z = 648 [M + H]^+$ 100%; 547 $[M - C_2Ph - H]^+$ 56%. 1H NMR ($CDCl_3$, δ): at 15 °C, 7.23, 7.14, 7.00 (m, Ph, 10H); 2.07 (m, PCH_2CH_3 , 6H); 1.95 (s, Cp^* , 15 H); 1.18 (m, PCH_2CH_3 , 9H). ^{13}C NMR ($CDCl_3$, δ): at 15 °C, 131.4 (s, $o-C$, Ph); 130.0 (s, $i-C$, Ph); 127.5 (s, $m-C$, Ph); 123.9 (s, $p-C$, Ph); 98.7 (s br, C_β , $-C\equiv CR$); 95.3 (s br, C_5Me_5); 80.2 (d br, $^2J_{P-C}$ 14.6, C_α , $-C\equiv CR$); 17.5 (d, $^1J_{P-C}$ 36.7, PCH_2CH_3); 9.4 (s, $C_5(CH_3)_5$); 7.8 (d, $^2J_{P-C}$ 3.5, PCH_2CH_3). ^{31}P NMR ($CDCl_3$, δ): at 15 °C, -8.5 (s).

Preparation of $[Cp^*Ir(C\equiv CSiMe_3)_2(PEt_3)]$ (4c**).** This complex was prepared by following a procedure similar to that for complexes **3** by treating $[Cp^*IrI_2(PEt_3)]$ (0.25 g, 0.36 mmol) with an excess of $LiC\equiv CSiMe_3$ (5.36 mmol, molar ratio 1:15). The reaction time was 4 h. The final residue was extracted with 30 mL of a toluene/hexane (1/1) mixture, and the extracts were filtered. The filtrate was evaporated to dryness, yielding **4c** as a cream-colored solid. Yield: 90%.

This complex can also be prepared, by a similar workup, starting from $[Cp^*IrCl_2(PEt_3)]$ (0.2 g, 0.39 mmol) and $LiC\equiv CSiMe_3$ (3.87 mmol, molar ratio 1:10) with a reaction time of 1 h. Yield: 85%.

Anal. Calcd for $C_{26}H_{48}IrPSi_2$: C, 48.79; H, 7.56. Found: C, 48.56; H, 7.65. MS: $m/z = 640 [M]^+$ 100%; 543 $[M - C_2SiMe_3]^+$ 60%; 521 $[M - 2C_2SiMe_3]^+$ 45%. 1H NMR ($CDCl_3$, δ): at 15

°C, 2.00 (m, PCH_2CH_3 , 6H); 1.83 (d, $^4J_{P-H}$ 1.1, Cp^* , 15 H); 1.06 (dt, $^3J_{P-H}$ 15.7, $^3J_{H-H}$ 7.9, PCH_2CH_3 , 9H); 0.01 (s, $SiMe_3$, 18H). ^{13}C NMR ($CDCl_3$, δ): at -50 °C, 104.35 (d, $^2J_{P-C}$ 18.37, C_α , $-C\equiv CR$); 100.30 (d, $^3J_{P-C}$ 0.7, C_β , $-C\equiv CR$); 94.79 (d, $^2J_{P-C}$ 2.4, C_5Me_5); 16.86 (d, $^1J_{P-C}$ 37.1, PCH_2CH_3); 9.12 (d, $^3J_{P-C}$ 0.6, $C_5(CH_3)_5$); 7.59 (d, $^2J_{P-C}$ 3.5, PCH_2CH_3); 1.56 (s, $SiMe_3$). ^{31}P NMR ($CDCl_3$, δ): at 15 °C, -9.2 (s); at -50 °C, -8.2 (s).

Preparation of $[(PEt_3)Cp^*Rh(\mu-C\equiv CPh)_2Pt(C_6F_5)_2]$ (5a**). Method A.** A solution of $[Cp^*RhCl_2(PEt_3)]$ (0.073 g, 0.17 mmol) in acetone (10 mL) was treated with $AgClO_4$ (0.0705 g, 0.34 mmol), and the mixture was stirred at room temperature for 1 h. The $AgCl$ was filtered and the filtrate treated with $[PMePh_3]_2[Pt(C_6F_5)_2(C\equiv CPh)_2]$ (0.2 g, 0.16 mmol). The mixture was stirred for 15 min and evaporated to dryness, and then treatment of the residue with $EtOH$ afforded complex **5a** as an orange solid. Yield: 28%.

Method B. $[Pt(C_6F_5)_2(thf)_2]$ (0.11 g, 0.17 mmol) was added to a solution of $[Cp^*Rh(C\equiv CPh)_2(PEt_3)]$ (**3a**; 0.095 g, 0.17 mmol) in CH_2Cl_2 (15 mL). The mixture was stirred for 3 min, and the resulting red solution was evaporated to dryness. Addition of 5 mL of Et_2O rendered **5a** as an orange solid. Yield: 41%.

Data for **5a**: Anal. Calcd for $C_{44}H_{40}F_{10}P_2Rh$: C, 48.59; H, 3.71. Found: C, 48.44; H, 3.76. MS: $m/z = 919 [M - C_6F_5 - H]^+$ 8%; 558 $[Cp^*Rh(C_2Ph)(PEt_3)]^+$ 20%; 457 $[Cp^*Rh(C_2Ph)(PEt_3)]^+$ 10%; 441 $[Cp^*Rh(C_2Ph) - H]^+$ 21%; 356 $[Cp^*Rh(PEt_3)]^+$ 100%. 1H NMR ($CDCl_3$, δ): at 15 °C, 7.22, 6.88 (m, Ph, 10H); 1.99 (d, $^4J_{P-H}$ 2.68, Cp^* , 15 H); 1.87 (m, PCH_2CH_3 , 6H); 1.03 (m, PCH_2CH_3 , 9H). The ^{13}C NMR spectrum could not be obtained due to decomposition. ^{19}F NMR ($CDCl_3$, δ): at 15 °C, -118 (v br, 4 $o-F$); -165.0 (t, 2 $p-F$); -166.3 (m, 4 $m-F$); at -50 °C, -117.4 (d, $^3J_{Pt-o-F}$ 441, 2 $o-F$); -119.63 (d, $^3J_{Pt-o-F}$ 353, 2 $o-F$); -164.3 (t, 2 $p-F$); -165.5 (m, 2 $m-F$); -165.9 (m, 2 $m-F$). ^{31}P NMR ($CDCl_3$, δ): at 15 °C, 32.1 (d, $^1J_{P-Rh}$ 128).

Preparation of $[(PEt_3)Cp^*Rh(\mu-C\equiv CSiMe_3)_2Pt(C_6F_5)_2]$ (5c**). Method A.** $[NBu_4][Pt(C_6F_5)_2(C\equiv CSiMe_3)_2]$ (0.2 g, 0.16 mmol) was added to a filtered solution of $[Cp^*Rh(PEt_3)(acetone)]_2(ClO_4)_2$ (0.17 mmol) in 20 mL of acetone, prepared from 72 mg (0.17 mmol) of $[Cp^*RhCl_2(PEt_3)]$ and 70 mg (0.34 mmol) of $AgClO_4$, and the resulting deep orange solution was stirred for 5 min. The solution was partially evaporated, causing the precipitation of complex **5c** as an orange microcrystalline solid. Yield: 62%.

Method B. A solution of $[Cp^*Rh(C\equiv CSiMe_3)_2(PEt_3)]$ (**3c**; 0.23 g, 0.41 mmol) in 15 mL of CH_2Cl_2 was treated with $[Pt(C_6F_5)_2(thf)_2]$ (0.2 g, 0.3 mmol). After 3 min of stirring the resulting solution was concentrated to ca. 3 mL and complex **5c** was separated as an orange solid, which was filtered off and washed with $EtOH$. Yield: 41%.

Data for **5c**: Anal. Calcd for $C_{38}H_{48}F_{10}P_2RhSi_2$: C, 42.26; H, 4.47. Found: C, 42.24; H, 4.91. MS: $m/z = 1081 [M + H]^+$ 3%; 551 $[Cp^*Rh(C_2SiMe_3)_2(PEt_3)]^+$ 27%; 431 $[Cp^*Rh(C_2SiMe_3)_2 - H]^+$ 100%; 356 $[Cp^*Rh(PEt_3)]^+$ 62%. FAB(-): m/z 961 $[M - (PEt_3)]^-$ 30%; 926 $[Pt(C_6F_5)_2(C_2SiMe_3)]^-$ 100%. 1H NMR (acetone- d_6 , δ): at 15 °C, 2.10 (m, PCH_2CH_3 , 6H); 1.95 (d, $^4J_{P-H}$ 2.3, Cp^* , 15 H); 1.23 (m, PCH_2CH_3 , 9H); 0.00 (s, $SiMe_3$, 18H); at -50 °C, 2.06 (m, PCH_2CH_3 , 6H); 1.92 (d, $^4J_{P-H}$ 1.3, Cp^* , 15 H); 1.20 (m, PCH_2CH_3 , 9H); -0.04 (s, $SiMe_3$, 18H); at -90 °C the signals are broad, 1.9 (d, Cp^*), 1.16 (m, PCH_2CH_3), -0.06 (br, $SiMe_3$). ^{13}C NMR (acetone- d_6 , δ): at -50 °C, due to the low solubility of this complex, the C_α and C_β signals are not seen; 149.5, 146.6, 137.9, 134.7 (br, C_6F_5); 104.80 (dd, $^1J_{Rh-C}$ 4.74, $^2J_{P-C}$ 2.41, C_5Me_5); 19.52 (d, $^1J_{P-C}$ 29.2, PCH_2CH_3); 10.17 (s, $C_5(CH_3)_5$); 9.12 (d, $^2J_{P-C}$ 6.3, PCH_2CH_3); 1.53 (s, $SiMe_3$, $C\equiv CR$). ^{19}F NMR (acetone- d_6 , δ): at 15 °C, -114.0 (d, $^3J_{Pt-o-F}$ 454, 2 $o-F$); -116.3 (d, $^3J_{Pt-o-F}$ 410, 2 $o-F$); -166.1 (t, 2 $p-F$); -166.8 (m, 4 $m-F$); at -50 °C, -113.9 (d, $^3J_{Pt-o-F}$ 460, 2 $o-F$); -116.3 (s br, $^3J_{Pt-o-F}$ 394, 2 $o-F$); -165.3 (t, 2 $p-F$); -166.0 (m, 4 $m-F$); at -90 °C, -113.8 (br, $^3J_{Pt-o-F} \approx 480$, 2 $o-F$); -117.5 (coalesces, 2 $o-F$); -164.7 (t, 2 $p-F$); -165.6

(br, 4 *m*-F). ^{31}P NMR (acetone- d_6 , δ): at 15 °C, 31.7 (d, $^1J_{\text{P-Rh}}$ 130); at -90 °C, 31.8 (d, $^1J_{\text{P-Rh}}$ 129).

Preparation of [(PEt₃)Cp*Rh(μ -C \equiv CR)₂Pd(C₆F₅)₂] (R = Ph (6a), SiMe₃ (6c)). [*cis*-Pd(C₆F₅)₂(thf)₂] (0.12 g, 0.205 mmol) was added to a solution of [Cp*Rh(C \equiv CPh)₂(PEt₃)] (3a; 0.115 g, 0.205 mmol) in diethyl ether (20 mL) at -20 °C. The resulting solution was immediately concentrated to a small volume (ca. 5 mL), causing the precipitation of 6a as a dark orange solid, which was filtered off and washed with Et₂O (ca. 2 mL). Yield: 70%.

Complex 6c was prepared in a way similar to that for 6a, starting from 3c (0.45 g, 0.81 mmol) and [*cis*-Pd(C₆F₅)₂(thf)₂] (0.74 mmol). Reaction time: 5 min. Yield: 36%.

Data for 6a: Anal. Calcd for C₄₄H₄₀F₁₀PPdRh: C, 52.9; H, 4.03. Due to its instability in solution 6a is probably impure, due to the presence of traces of Pd. The best analyses found: C, 51.88; H, 3.72. MS: *m/z* = 1082 [Pd₂(C₆F₅)₄(C₂Ph)₂]⁺ 10%; 998 [M]⁺ 24%, 880 [M - (PEt₃)]⁺ 80%; 642 [Pd(C₆F₅)₂(C₂Ph)₂]⁺ 92%; 356 [Cp*Rh(PEt₃)]⁺ 100%, 325 [Rh(C₂Ph)(PEt₃) + 3H]⁺ 90%. This complex is very unstable and was characterized only at -50 °C. ^1H NMR (CDCl₃, δ): at -50 °C, 7.09, 7.02, 6.93 (m, Ph, 10H); 2.03 (s br, Cp*, PCH₂CH₃, 21H); 1.04 (m, PCH₂CH₃, 9H). ^{19}F NMR (CDCl₃, δ): at -50 °C, -114.0 (d, 2 *o*-F); -116.4 (d, 2 *o*-F); -163.4 (t, 2 *p*-F); -163.6 (m, 2 *m*-F); -165.1 (m, 2 *m*-F). ^{31}P NMR (CDCl₃, δ): at -50 °C, 35.6 (d, $^1J_{\text{P-Rh}}$ 123). Due to the very low stability of this complex in solution, its ^{13}C NMR spectrum could not be registered.

Data for 6c: Anal. Calcd for C₃₈H₄₈F₁₀PPdRhSi₂: C, 46.00; H, 4.90. Found: C, 45.65; H, 5.30. MS: *m/z* = 657 [Cp*Rh-(C₂SiMe₃)₂(PEt₃)Pd]⁺ 21%; 539 [Pd(C₆F₅)₂(C₂SiMe₃) + 2H]⁺ 21%; 433 [Cp*Rh(CCSiMe₃)₂ + H]⁺ 63%; 356 [Cp*Rh(PEt₃)]⁺ 73%. ^1H NMR (acetone- d_6 , δ): at 15 °C, 2.09 (m, PCH₂CH₃, 6H); 2.05 (d, $^4J_{\text{P-H}}$ 2.1, 15 H, Cp*); 1.23 (m, PCH₂CH₃, 9H); -0.18 (s, SiMe₃, 18H); at -50 °C, 2.06 (m, Cp*, PCH₂CH₃, 21H); 1.16 (m, PCH₂CH₃, 9H); -0.23 (s, SiMe₃, 18H); at -90 °C, 2.06 (m, PCH₂CH₃, 6H); 2.02 (s, 15 H, Cp*); 1.11 (m, PCH₂CH₃, 9H); -0.27 (s, SiMe₃, 18H). ^{19}F NMR (acetone- d_6 , δ): at 15 °C, -109.9 (m, 2 *o*-F); -113.3 (m, 2 *o*-F); -164.3 (t, 2 *p*-F); -165.6 (m, 4 *m*-F); at -50 °C, -109.5 (d, 2 *o*-F); -113.2 (d, 2 *o*-F); -163.5 (t, 2 *p*-F); -164.9 (m, 4 *m*-F); the same pattern was observed at -90 °C, -109.3 (d, 2 *o*-F); -113.0 (d, 2 *o*-F); -162.9 (t, 2 *p*-F); -164.4 (m, 4 *m*-F). ^{31}P NMR (acetone- d_6 , δ): at 15 °C, 33.2 (d, $^1J_{\text{P-Rh}}$ 125); at -50 °C, 34.1 (d, $^1J_{\text{P-Rh}}$ 125); at -90 °C, 34.8 (d, $^1J_{\text{P-Rh}}$ 125.5). Due to the low solubility and stability in solution the ^{13}C NMR spectrum could not be registered.

Preparation of [(PEt₃)Cp*Ir(μ -C \equiv CR)₂Pt(C₆F₅)₂] (R = Ph (7a), SiMe₃ (7c)). Method A. The preparation of 7a starting from [PMePh₃][*cis*-Pt(C₆F₅)₂(C \equiv CPh)₂] and [Cp*Ir-(PEt₃)₂(acetone)]₂(ClO₄)₂ (prepared from [Cp*IrCl₂(PEt₃)] and AgClO₄) has been previously described.¹⁴ Yield: 62%.

Complex 7c was prepared by following the synthesis described in method A for complex 5c, but starting from an acetone solution which contains 0.16 mmol of [Cp*Ir(PEt₃)₂(acetone)]₂(ClO₄)₂ and 0.2 g (0.16 mmol) of [NBu₄][*cis*-Pt(C₆F₅)₂(C \equiv CSiMe₃)₂]. Yield: 32%.

Method B. Both yellow complexes can also be prepared as described in method B for complex 5a, but starting from [Cp*Ir(C \equiv CR)₂(PEt₃)] (R = Ph (4a), 0.094 g, 0.14 mmol; R = SiMe₃ (4c), 0.090 g, 0.14 mmol) and [*cis*-Pt(C₆F₅)₂(thf)₂] (0.097 g, 0.14 mmol) and stirring for 5 min. Yield: 64.5% for 7a and 35% for 7c.

Data for 7a: Anal. Calcd for C₄₄H₄₀F₁₀IrPPt: C, 44.9; H, 3.42. Found: C, 44.55; H, 3.22. MS: *m/z* = 1176 [M]⁺ 10%, 648 [Cp*Ir(C₂Ph)₂(PEt₃)]⁺ 12%; 547 [Cp*Ir(C₂Ph)(PEt₃)]⁺ 14%; 310 [Ir(PEt₃)]⁺ 100%. ^1H NMR (CDCl₃, δ): at 20 °C, 7.06 (m, Ph, 10 H); 2.16 (d, $^4J_{\text{P-H}}$ 1.9, Cp*, 15 H); 1.95 (m, PCH₂CH₃, 6H); 0.96 (m, PCH₂CH₃, 9H); in acetone- d_6 , at -90 °C, 7.13, 7.05 (m, Ph, 10 H); 2.07 (m, Cp*, PCH₂CH₃, 21 H); 0.88 (m, PCH₂CH₃, 9H). ^{13}C NMR (CDCl₃, δ): at 20 °C, 147.8, 144.75, 137.4, 134.2 (m br, C₆F₅); 130.9, 126.9 (s, Ph); 126.5 (s br, *p*-C,

Ph); 125.5 (s, *i*-C, Ph); 98.0 (s, C _{β} , -C \equiv CR); 97.8 (d, $^2J_{\text{C-P}}$ 2.6, C₅Me₃); 55.3 (d, $^2J_{\text{P-C}}$ 17, C _{α} , -C \equiv CR); 14.7 (d, $^1J_{\text{P-C}}$ 36, PCH₂CH₃); 9.3 (s, C₅(CH₃)₅); 6.7 (d, $^2J_{\text{P-C}}$ 2.8, PCH₂CH₃). ^{19}F NMR (CDCl₃, δ): at 20 °C, -114.9 (s br, 2 *o*-F), -119.3 (s br, 2 *o*-F) (platinum satellites due to $^3J_{\text{Pt-o-F}}$ are observed but are not well-resolved); -164.9 (t, 2 *p*-F); -165.9, -166.5 (s br, 4 *m*-F, overlapped); at -50 °C, -113.2 (d br, $^3J_{\text{Pt-o-F}}$ 389, 2 *o*-F); -117.81 (dd, $^3J_{\text{Pt-o-F}}$ 425, 2 *o*-F); -165.1 (t, 2 *p*-F); -165.7 (m, 2 *m*-F); -166.3 (m, 2 *m*-F); in acetone- d_6 , at -90 °C, -113.3 (s br, $^3J_{\text{Pt-o-F}}$ 387, 2 *o*-F); -117.7 (d, $^3J_{\text{Pt-o-F}}$ 391, 2 *o*-F); -164.4 (t, 2 *p*-F); -165.3 (m, 2 *m*-F); -165.7 (m, 2 *m*-F). ^{31}P NMR (acetone- d_6 , δ): at 20 °C, 5.8 (s); at -90 °C, 2.3 (s).

Data for 7c: Anal. Calcd for C₃₈H₄₈F₁₀IrPPtSi₂: C, 39.03; H, 4.14. Found: C, 38.81; H, 3.95. MS: *m/z* = 1169 [M]⁺ 7%; 640 [Cp*Ir(C₂SiMe₃)₂(PEt₃)]⁺ 100%; 626 [Pt(C₆F₅)₂(C₂SiMe₃)]⁺ 47%; 543 [Cp*Ir(C₂SiMe₃)₂(PEt₃)]⁺ 62%. ^1H NMR (CDCl₃, δ): at 15 °C, 2.06 (d, $^4J_{\text{P-H}}$ 1.7, Cp*, 15 H); 1.98 (m, PCH₂CH₃, 6H); 1.10 (m, PCH₂CH₃, 9H); -0.18 (s, SiMe₃, 18H); a similar pattern was observed at -50 °C with only a singlet at δ -0.24 due to SiMe₃; an identical pattern was seen in acetone- d_6 even at -85 °C (δ SiMe₃ -0.2). ^{13}C NMR (acetone- d_6 , δ): at -50 °C, 148.4, 145.1, 137.5, 134.4 (br, C₆F₅); 98.09 (d, $^2J_{\text{P-C}}$ 2.3, C₅Me₃); 93.77 (ill-defined signal C _{α} or C _{β}); 16.86 (d, $^1J_{\text{P-C}}$ 35.12, PCH₂CH₃); 9.5 (s, C₅(CH₃)₅); 8.25 (d, $^2J_{\text{P-C}}$ 4.05, PCH₂CH₃); 0.92 (s, SiMe₃, C \equiv CR). ^{19}F NMR (CDCl₃, δ): at 15 °C, -113.3 (m br, 2 *o*-F); -117.5 (m br, 2 *o*-F); -164.7 (t, 2 *p*-F); -166.1 (m, 4 *m*-F); at -50 °C, -113.6 (d, $^3J_{\text{Pt-o-F}}$ 462, 2 *o*-F); -117.9 (d, $^3J_{\text{Pt-o-F}}$ 432, 2 *o*-F); -164.1 (t, 2 *p*-F); -165.3 (m, 2 *m*-F); -165.8 (m, 2 *m*-F); a similar pattern was observed in acetone- d_6 , but in this solvent the *m*-F resonances did not resolve into separate signals even at -85 °C, -112.0, -116.4 (*o*-F); -164.6 (t, *p*-F); -165.5 (*m*-F); on heating, only the 2 *o*-F resonances broadened at ca. 0 °C, they still were broad at 16 °C, and they finally coalesced at 40 °C. ^{31}P NMR (CDCl₃, δ): at 15 °C, -5.1 (s); at -50 °C, -4.3(5).

Preparation of [(PEt₃)Cp*Ir(μ -C \equiv CR)₂Pd(C₆F₅)₂] (R = Ph (8a), SiMe₃ (8c)). 8a. [*cis*-Pd(C₆F₅)₂(thf)₂] (0.14 g, 0.25 mmol) was added to a cooled (-20 °C) solution of [Cp*Ir(C \equiv CPh)₂(PEt₃)] (4a; 0.16 g, 0.25 mmol) in CH₂Cl₂ (10 mL). The solution was immediately treated with charcoal and filtered through Celite and the filtrate evaporated to dryness. Addition of cold Et₂O to the residue gave 8a as a yellow solid. Yield: 62%.

8c. Complex 8c was obtained as a beige solid in a way similar to that for complex 8a, starting from 4c (0.1 g, 0.16 mmol) and [*cis*-Pd(C₆F₅)₂(thf)₂] (0.097 g, 0.16 mmol). Yield: 38%.

Data for 8a: Anal. Calcd for C₄₄H₄₀F₁₀IrPPd: C, 48.56; H, 3.70. Found: C, 48.35; H, 3.98. MS: *m/z* = 1088 [M]⁺ 13%; 754 [Cp*Ir(C₂Ph)₂(PEt₃)Pd]⁺ 100%; 649 [Cp*Ir(C₂Ph)₂(PEt₃)]⁺ 26%; 548 [Cp*Ir(C₂Ph)(PEt₃)]⁺ 24%. ^1H NMR (CDCl₃, δ): at 16 °C, 7.03, 6.91 (m, Ph, 10H); 2.14 (s, Cp*, 15H); 2.10 (m, PCH₂CH₃, 6 H); 1.04 (dt, $^3J_{\text{H-P}}$ 16.1, $^3J_{\text{H-H}}$ 8.19, PCH₂CH₃, 9H); at -50 °C, a similar spectrum was observed but with broader signals. ^{13}C NMR (CDCl₃, δ): at -50 °C, 146.6, 143.5, 136.8, 133.23 (br, C₆F₅); 131.41 (s, *o*-C, Ph); 127.1 (s, *m*-C, Ph); 126.57 (s), 125.13 (s) (*p*-C and *i*-C, Ph); 100.52 (s, probably due to C _{β} , -C \equiv CR); 96.98 (s, C₅Me₃); 51.29 (d, $^2J_{\text{P-C}}$ \approx 18, C _{α} , -C \equiv CR); 15.07 (d, $^1J_{\text{P-C}}$ \approx 40, PCH₂CH₃); 9.55 (s, C₅(CH₃)₅); 7.14 (d, $^2J_{\text{P-C}}$ 3.0, PCH₂CH₃); signals at 15.3 and 66.08 due to diethyl ether are also observed. ^{19}F NMR (CDCl₃, δ): at 15 °C, -113.7 (d, 2 *o*-F); -116.3 (d, 2 *o*-F); -163.9 (m, 2 *m*-F, 2 *p*-F); -165.7 (m, 2 *m*-F); at -50 °C, -113.9 (d, 2 *o*-F); -116.2 (d, 2 *o*-F); -163.3 (t, 2 *p*-F); -163.7 (m, 2 *m*-F); -165.1 (m, 2 *m*-F). ^{31}P NMR (CDCl₃, δ): at 15 °C, -6.2 (s); at -50 °C, 4.7 (s).

Data for 8c: Anal. Calcd for C₃₈H₄₈F₁₀IrPPdSi₂: C, 42.24; H, 4.48. Found: C, 41.88; H, 3.96. MS: *m/z* = 640 [Cp*Ir-(C₂SiMe₃)₂(PEt₃) + H]⁺ 100%; 543 [Cp*Ir(C₂SiMe₃)₂(PEt₃) + H]⁺ 53%; 446 [Cp*Ir(PEt₃) + H]⁺ 59%; 385 [Ir(C₂SiMe₃) + H]⁺ 68%. ^1H NMR (CDCl₃, δ): at 15 °C, 2.05 (s, Cp*, 15H); \sim 2.01 (m,

PCH_2CH_3 , 6 H); 1.12 (m, PCH_2CH_3 , 9H); -0.23 (s, SiMe_3 , 18H). ^{19}F NMR (CDCl_3 , δ): at -50°C , -111.1 (d, 2 *o*-F); -114.6 (d, 2 *o*-F); -162.6 (t, 2 *p*-F); -164.2 (m, 2 *m*-F); -164.8 (m, 2 *m*-F); at 16°C , -111.1 (br, 2 *o*-F); -114.5 (br, 2 *o*-F); -163.2 (t, 2 *p*-F); -165.0 (br, 4 *m*-F). The *o*-F signals coalesce at $\sim 30^\circ\text{C}$. ^{31}P NMR (CDCl_3 , δ): at 15°C , -8.6 (s). The ^{13}C NMR spectrum could not be obtained due to the low stability of complex **8c** in solution even at low temperature.

Preparation of [(PEt₃)Cp*Rh(μ -C≡CR)(μ -Cl)Pt(C₆F₅)₂] (R = Ph (9a), ^tBu (9b)). **9a.** [*cis*-Pt(C₆F₅)₂(thf)₂] (0.21 g, 0.32 mmol) was added to a solution of [Cp*Rh(C≡CPh)Cl(PEt₃)] (**1a**) with **3a** ($\sim 14\%$) and [Cp*RhCl₂(PEt₃)] ($\sim 12\%$) (0.16 g, ~ 0.32 mmol) as impurities in 10 mL of CH₂Cl₂, and the mixture was stirred for 5 min. The resulting solution was evaporated to dryness and the solid residue treated with cold Et₂O (ca. 5 mL), affording an orange solid which was identified as **9a**: CH₂Cl₂. Yield: 36%.

9b. Complex **9b** can be obtained as described for complex **9a**, but starting from 0.13 g (0.28 mmol) of [Cp*Rh(C≡C^tBu)Cl(PEt₃)] (**1b**) and 0.19 g (0.28 mmol) of [*cis*-Pt(C₆F₅)₂(thf)₂]. Yield: 61%.

Data for **9a**: Anal. Calcd for C₃₇H₃₇Cl₃F₁₀PPtRh: C, 38.71; H, 3.34. Found: C, 39.06; H, 3.47. MS: $m/z = 985$ [M - Cl - 2H]⁺ 9%; 665 [Pt(C₆F₅)₂Cl(C₂Ph)]⁺ 45%; 391 [Cp*RhCl(PEt₃)]⁺ 82%; 355 [Cp*Rh(PEt₃) - H]⁺ 71%. ^1H NMR (CDCl_3 , δ): at 15°C , 7.13, 7.04 (m, Ph, 5 H); 5.29 (s, CH₂Cl₂, 2H); 2.01 (m, PCH₂CH₃, 6H); 1.89 (d, ⁴J_{P-H} 2.7, Cp*, 15 H); 1.05 (m, PCH₂CH₃, 9H). ^{19}F NMR (CDCl_3 , δ): at 15°C , -117.2 (d, ³J_{Pt-o-F} 512, 1 *o*-F); -119.6 (overlapping of two *o*-F); -120.4 (d, ³J_{Pt-o-F} 466, 1 *o*-F); -162.9 (t, 1 *p*-F); -165.2 (t, 1 *p*-F); -165.8 (m, 1 *m*-F); -166.0 (m, 1 *m*-F); -166.6 (m, 1 *m*-F); -167.0 (m, 1 *m*-F). ^{31}P NMR (CDCl_3 , δ): at 15°C , 33.5 (d, ¹J_{P-Rh} 134). The ^{13}C NMR spectrum could not be registered due to its very low solubility.

Data for **9b**: Anal. Calcd for C₃₄H₃₉ClF₁₀PPtRh: C, 40.75; H, 3.92. Found: C, 40.64; H, 3.44. MS: $m/z = 835$ [M - C₆F₅ + H]⁺ 8%; 437 [Cp*Rh(C₂Bu)(PEt₃)]⁺ 65%; 391 [Cp*RhCl(PEt₃)]⁺ 73%; 356 [Cp*Rh(PEt₃)]⁺ 52%. ^1H NMR (CDCl_3 , δ): at 15°C , 2.04 (m, PCH₂CH₃, 6H); 1.84 (d, ⁴J_{P-H} 2.9, Cp*, 15 H); 1.16 (m, PCH₂CH₃, 9H); 0.90 (s, ^tBu, 9 H). ^{19}F NMR (CDCl_3 , δ): at 15°C , -116.0 (d, ³J_{Pt-o-F} 535, 1 *o*-F); -117.9 (d, ³J_{Pt-o-F} \approx 500, 1 *o*-F); -119.6 (d, ³J_{Pt-o-F} \approx 430, 1 *o*-F); -121.3 (d, ³J_{Pt-o-F} \approx 440, 1 *o*-F); -163.2 (t, 1 *p*-F); -164.3 (t, 1 *p*-F); -165.15 (m, 1 *m*-F); -165.8 (m, overlapping of two *m*-F); -166.9 (m, 1 *m*-F). ^{31}P NMR (CDCl_3 , δ): at 15°C , 30.7 (d, ¹J_{P-Rh} 136). The ^{13}C NMR spectrum could not be obtained due to the low solubility of the complex.

Preparation of a Mixture of [(PEt₃)Cp*Rh(μ -C≡CSiMe₃)(μ -Cl)Pt(C₆F₅)₂] (9c) and (5c). Starting from a mixture of 0.25 g of complexes **1c** and **3c** in a 2:1 ratio (0.327 mmol for **1c** and 0.163 mmol for **3c**) and 0.33 g (0.49 mmol) of [*cis*-Pt(C₆F₅)₂(thf)₂] and following the procedure described for the synthesis of compound **9a**, a mixture of complexes **9c** and **5c** in a ca. 4:1 ratio was obtained as an orange microcrystalline solid (0.23 g). All attempts to obtain pure **9c** from this mixture were unsuccessful; therefore, complex **9c** was only spectroscopically characterized from the mixture.

Data for **9c**: ^1H NMR (CDCl_3 , δ): at 15°C , 2.04 (m, PCH₂CH₃, 6H); 1.84 (d, ⁴J_{P-H} 2.8, Cp*, 15 H); 1.13 (m, PCH₂CH₃, 9H); -0.17 (s, SiMe₃, 9 H). ^{19}F NMR (CDCl_3 , δ): at 15°C , -115.7 (d, ³J_{Pt-o-F} \approx 545, 1 *o*-F); -118.3 (d, ³J_{Pt-o-F} \approx 470, 1 *o*-F); -119.5 (d, ³J_{Pt-o-F} \approx 450, 1 *o*-F); -121.0 (d, ³J_{Pt-o-F} \approx 460, 1 *o*-F); -163.2 (t, 1 *p*-F); -164.5 (t, 1 *p*-F); -165.2 (m, 1 *m*-F); -165.8 (m, 1 *m*-F); -166.2 (m, 1 *m*-F); -166.7 (m, 1 *m*-F). ^{31}P NMR (CDCl_3 , δ): at 15°C , 32.1 (d, ¹J_{P-Rh} 135).

Preparation of [(PEt₃)Cp*Rh(μ -C≡CPh)(μ -Cl)Pd(C₆F₅)₂] \cdot $\frac{1}{2}$ CH₂Cl₂ (10a \cdot $\frac{1}{2}$ CH₂Cl₂). Complex **10a**, which crystallizes with a half molecule of CH₂Cl₂ (^1H NMR), can be prepared by following the same procedure as for complex **9a** but starting from 0.16 g (~ 0.3 mmol) of [Cp*Rh(C≡CPh)Cl(PEt₃)] (**1a**;

impure sample) and 0.19 g (0.35 mmol) of [*cis*-Pd(C₆F₅)₂(thf)₂] at -20°C . Yield: 23%.

Data for **10a** \cdot $\frac{1}{2}$ CH₂Cl₂: Anal. Calcd for C_{36.5}H_{36.5}Cl₂F₁₀PPdRh: C, 44.92; H, 3.70. Found: C, 44.93; H, 3.50. MS: $m/z = 765$ [M - C₆F₅]⁺ 8%; 701 [M - Cp* - (PEt₃) + 2H]⁺ 12%; 457 [Cp*Rh(C₂Ph)(PEt₃)]⁺ 36%; 391 [Cp*RhCl(PEt₃)]⁺ 100%; 356 [Cp*Rh(PEt₃)]⁺ 40%. ^1H NMR (CDCl_3 , δ): at 15°C , 7.25, 7.05 (m, Ph, 5 H); 5.29 (s, CH₂Cl₂, 1 H); 1.96 (m, PCH₂CH₃, 6H); 1.90 (d, ⁴J_{P-H} 2.7, Cp*, 15 H); 1.12 (m, PCH₂CH₃, 9H). ^{19}F NMR (CDCl_3 , δ): at 15°C , -114.6 (d, 1 *o*-F); -116.2 (d, 1 *o*-F); -116.7 (m, overlapping of 2 *o*-F); -162.2 (t, 1 *p*-F); -163.7 (t, 1 *p*-F); -164.2 (m, 1 *m*-F); -164.8 (m, overlapping of 2 *m*-F); -165.6 (m, 1 *m*-F). ^{31}P NMR (CDCl_3 , δ): at 15°C , 31.9 (d, ¹J_{P-Rh} 132). Due to its very low solubility and stability in solution, the ^{13}C NMR spectrum could not be registered.

Preparation of [(PEt₃)Cp*Rh(μ -C≡C^tBu)(μ -Cl)Pd(C₆F₅)₂] (10b). A 0.198 g (0.338 mmol) portion of [*cis*-Pd(C₆F₅)₂(thf)₂] was added to a cooled (-20°C) dichloromethane solution of **1b** (0.16 g, 0.338 mmol). The resulting brown solution was treated with C_{active} and, immediately, filtered through Celite. Evaporation to dryness of the filtrate, followed by addition of cold diethyl ether, yielded **10b** as an orange solid. Yield: 58%.

Data for **10b**: Anal. Calcd for C₃₄H₃₉ClF₁₀PPdRh: C, 44.71; H, 4.30. Found: C, 44.62; H, 4.38. MS: $m/z = 699$ [M - Cp* - C₂Bu + H]⁺ 19%; 519 [Pd(C₆F₅)₂(C₂Bu) - 2H]⁺ 26%; 437 [Cp*Rh(C₂Bu)(PEt₃)]⁺ 76%; 391 [Cp*RhCl(PEt₃)]⁺ 46%; 356 [Cp*Rh(PEt₃)]⁺ 42%. ^1H NMR (CDCl_3 , δ): at 15°C , 2.08 (m, PCH₂CH₃, 6H); 1.85 (d, ⁴J_{P-H} 2.8, Cp*, 15 H); 1.17 (m, PCH₂CH₃, 9H); 0.85 (s, ^tBu, 9 H). ^{19}F NMR (CDCl_3 , δ): at 15°C , -112.6 (d, 1 *o*-F); -113.6 (d, 1 *o*-F); -116.4 (d, 1 *o*-F); -118.2 (d, 1 *o*-F); -162.3 (m, overlapping of two *p*-F); -164.4 (m, 1 *m*-F); -164.6 (m, 1 *m*-F); -164.9 (m, 1 *m*-F); -165.5 (m, 1 *m*-F). ^{31}P NMR (CDCl_3 , δ): at 15°C , 29.5 (d, ¹J_{P-Rh} 133). The complex is not soluble enough for ^{13}C NMR.

Preparation of [(PEt₃)Cp*Ir(μ -C≡CPh)(μ -Cl)Pt(C₆F₅)₂] (11a). A suspension of [Cp*Ir(C≡CPh)Cl(PEt₃)] (**4a**; 0.09 g, 0.15 mmol) in 10 mL of CH₂Cl₂ was treated with [*cis*-Pt(C₆F₅)₂(thf)₂] (0.09 g, 0.14 mmol), immediately giving a dark orange solution, which was evaporated to ca. 2 mL. Addition of 3 mL of cold EtOH caused the precipitation of complex **11a** as a yellow solid. Yield: 86%.

Data for **11a**: Anal. Calcd for C₃₆H₃₅ClF₁₀IrPPt: C, 38.9; H, 3.17. Found: C, 38.5; H, 2.90. MS: $m/z = 1111$ [M]⁺ 6%; 1075 [M - Cl]⁺ 12%; 943 [M - C₆F₅ - H]⁺ 9%; 580 [Cp*Ir(C₂Ph)Cl(PEt₃) - H]⁺ 26%; 547 [Cp*Ir(C₂Ph)(PEt₃)]⁺ 39%; 481 [Cp*IrCl(PEt₃) + H]⁺ 56%; 411 [Ir(C₂Ph)(PEt₃)]⁺ 50%; 327 [Cp*Ir]⁺ 100%. ^1H NMR (CDCl_3 , δ): at 15°C , 7.12, 7.03 (m, Ph, 5 H); 2.06 (m, PCH₂CH₃, 6H); 1.96 (s br, Cp*, 15 H); 1.01 (dt, ³J_{P-H} 16.4, ³J_{H-H} 8.3, PCH₂CH₃, 9H). ^{19}F NMR (CDCl_3 , δ): at 15°C , -117.6 (d, ³J_{Pt-o-F} 520, 1 *o*-F); -119.97 , -120.07 (overlapping of two doublets, 2 *o*-F); -120.7 (d, ³J_{Pt-o-F} \approx 470, 1 *o*-F); -163.0 (t, 1 *p*-F); -165.2 (m, 1 *m*-F); -165.3 (t, 1 *p*-F); -165.9 (m, 1 *m*-F); -166.9 (m, 1 *m*-F); -167.2 (m, 1 *m*-F). ^{31}P NMR (CDCl_3 , δ): at 15°C , 1.3 (s). Due to the low solubility, the ^{13}C NMR spectrum could not be registered.

Preparation of [(PEt₃)Cp*Ir(μ -C≡CR)(μ -I)Pt(C₆F₅)₂] (R = Ph (11a'), SiMe₃ (11c')). **11a'**. A suspension of **2a'** (0.1 g, 0.15 mmol) in 10 mL of CH₂Cl₂ was treated with [*cis*-Pt(C₆F₅)₂(thf)₂] (0.1 g, 0.15 mmol) at low temperature and the mixture was stirred for 5 min. Evaporation of the resulting solution and addition of cold diethyl ether give **11a'** as a yellow microcrystalline solid. Yield: 66%.

11c'. Complex **11c'** was prepared as a yellow solid by following a procedure identical with that described for **11a'**: 0.16 g (0.24 mmol) of **2c'** and 0.16 g (0.24 mmol) of [*cis*-Pt(C₆F₅)₂(thf)₂] were used. Yield: 35%.

Data for **11a'**: Anal. Calcd for C₃₆H₃₅F₁₀IrPPt: C, 35.95; H, 2.93. Found: C, 35.79; H, 3.08. ES(-): m/z 1202 [M - H]⁻ 17%; 1067 [M - Cp*]⁻ 39%; 657 [Pt(C₆F₅)₂I]⁻ 100%. ^1H NMR (CDCl_3 , δ): at 15°C , 7.08 (2 H), 7.00 (3H) (m, Ph); 2.1 (m, PCH₂CH₃, 6H); 2.098 (d, ⁴J_{P-H} 1.5, Cp*, 15 H); 0.97 (dt, ³J_{P-H}

16, $^3J_{\text{H-H}}$ 8.2, PCH_2CH_3 , 9H). ^{19}F NMR (CDCl_3 , δ): at 15 °C, -116.8 (dd, $^3J_{\text{Pt-O-F}}$ 456, 1 *o*-F); -117.5 (dd, $^3J_{\text{Pt-O-F}} \approx 495$, 1 *o*-F); -118.8 (dd, $^3J_{\text{Pt-O-F}}$ 430, 1 *o*-F); -120.7 (dd, $^3J_{\text{Pt-O-F}}$ 435, 1 *o*-F); -163.2 (t, 1 *p*-F); -165.0 (t, 1 *p*-F); -165.1 (m, 1 *m*-F); -165.6 (m, 1 *m*-F); -166.3 (m, 1 *m*-F); -166.8 (m, 1 *m*-F). ^{31}P NMR (CDCl_3 , δ): at 15 °C, -5.7 (s). The complex is not soluble enough for ^{13}C NMR.

Data for **11c'**. Anal. Calcd for $\text{C}_{33}\text{H}_{39}\text{F}_{10}\text{IrPPtSi}$: C, 33.06; H, 3.28. Found: C, 33.28; H, 2.98. MS: $m/z = 669$ [$\text{Cp}^*\text{Ir}(\text{C}_2\text{SiMe}_3)\text{I}(\text{PET}_3)^+$] 18%; 573 [$\text{Cp}^*\text{Ir}(\text{PET}_3)^+$] 72%; 543 [$\text{Cp}^*\text{Ir}(\text{C}_2\text{SiMe}_3)(\text{PET}_3)^+$] 100%; 455 [$\text{Cp}^*\text{IrI} + \text{H}^+$] 59%; 443 [$\text{Cp}^*\text{Ir}(\text{PET}_3) - 2\text{H}^+$] 55%. ^1H NMR (CDCl_3 , δ): at 15 °C, 2.12 (m, PCH_2CH_3 , 6H); 2.05 (s, Cp^* , 15 H); 1.09 (m, PCH_2CH_3 , 9H); -0.17 (s, SiMe_3 , 9H). ^{19}F NMR (CDCl_3 , δ): at 15 °C, -116.0 (d, $^3J_{\text{Pt-O-F}}$ 524, 1 *o*-F); -116.6 (d, $^3J_{\text{Pt-O-F}}$ 470, 1 *o*-F); -118.2 (d, $^3J_{\text{Pt-O-F}}$ 454, 1 *o*-F); -120.1 (d, $^3J_{\text{Pt-O-F}}$ 453, 1 *o*-F); -163.6 (t, 1 *p*-F); -164.3 (t, 1 *p*-F); -165.4 (m, 1 *m*-F); -165.8 (m, 2 *m*-F); -166.6 (m, 1 *m*-F). ^{31}P NMR (CDCl_3 , δ): at 15 °C, -8.1 (s). A similar NMR pattern was observed at -50 °C. Due to the low solubility, its ^{13}C NMR spectrum could not be registered.

Preparation of [(PET₃)Cp*Ir(μ -C≡CPh)(μ -Cl)Pd(C₆F₅)₂] (12a). [*cis*-Pd(C₆F₅)₂(thf)₂] (0.12 g, 0.2 mmol) was added to a suspension of 0.12 g (0.2 mmol) of [$\text{Cp}^*\text{Ir}(\text{C}\equiv\text{CPh})\text{Cl}(\text{PET}_3)$] (**4a**) in 10 mL of CH_2Cl_2 at low temperature (-20 °C), and the mixture was stirred for 5 min. Evaporation of the mixture to ca. 2 mL caused the precipitation of a dark yellow-green solid which was recrystallized from $\text{CH}_2\text{Cl}_2/\text{Et}_2\text{O}$, giving **12a** as a yellow microcrystalline solid. Yield: 70%.

Data for **12a**. Anal. Calcd for $\text{C}_{36}\text{H}_{35}\text{ClF}_{10}\text{IrPPd}$: C, 42.28; H, 3.45. Found: C, 42.56; H, 3.62. MS: $m/z = 921$ [$\text{M} - \text{C}_2\text{Ph}$]⁺ 5%; 855 [$\text{M} - \text{C}_6\text{F}_5$]⁺ 5%; 754 [$\text{M} - \text{C}_6\text{F}_5 - \text{C}_2\text{Ph}$]⁺ 12%, 582 [$\text{Cp}^*\text{Ir}(\text{C}_2\text{Ph})\text{Cl}(\text{PET}_3)^+$] 7%; 547 [$\text{Cp}^*\text{Ir}(\text{C}_2\text{Ph})(\text{PET}_3)^+$] 29%. ^1H NMR (CD_2Cl_2 , δ): at 15 °C, 7.00, 6.90 (m, Ph, 5 H); 2.10 (m, PCH_2CH_3 , 6H); 1.94 (d, $^4J_{\text{P-H}}$ 1.7, Cp^* , 15 H); 1.02 (m, PCH_2CH_3 , 9H). ^{19}F NMR (CDCl_3 , δ): at 15 °C, -114.7 (d, 1 *o*-F); -116.6 (m, 3 *o*-F); -162.0 (t, 1 *p*-F); -163.6 (t, 1 *p*-F); -164.2 (m, 1 *m*-F); -164.8 (m, 2 *m*-F); -165.7 (m, 1 *m*-F). ^{31}P NMR (CDCl_3 , δ): at 15 °C, -2.4 (s). Due to the low solubility, the ^{13}C NMR spectrum could not be registered.

Preparation of [(PET₃)Cp*Ir(μ -C≡CR)(μ -I)Pd(C₆F₅)₂] (R = Ph (12a), SiMe₃ (12c')). These compounds were prepared as yellow solids in a way similar to that for complexes **11a'**, **c'**. A 0.12 g (0.18 mmol) portion of **2a'** and [*cis*-Pd(C₆F₅)₂(thf)₂] (0.104 g, 0.18 mmol) were used to prepare **12a'** (71% yield), and 0.11 g (0.16 mmol) of **2c'** with 0.096 g (0.16 mmol) of [*cis*-Pd(C₆F₅)₂(thf)₂] were used for the synthesis of **12c'** (yield 40%).

Data for **12a'**. Anal. Calcd for $\text{C}_{36}\text{H}_{35}\text{F}_{10}\text{IrPPd}$: C, 38.81; H, 3.17. Found: C, 39.07; H, 3.28. MS: $m/z = 947$ [$\text{M} - \text{C}_6\text{F}_5 + \text{H}^+$] 10%; 829 [$\text{M} - \text{C}_6\text{F}_5 - (\text{PET}_3) + \text{H}^+$] 12%; 573 [$\text{Cp}^*\text{IrI}(\text{PET}_3)^+$] 60%; 547 [$\text{Cp}^*\text{Ir}(\text{C}_2\text{SiMe}_3)(\text{PET}_3)^+$] 100%; 455 [$\text{Cp}^*\text{IrI} + \text{H}^+$] 54%. ^1H NMR (CDCl_3 , δ): at 15 °C, 6.99 (m, Ph, 5 H); 2.1 (m, PCH_2CH_3 , 6H); 2.13 (d, $^4J_{\text{P-H}}$ 1.1, Cp^* , 15 H); 1.00 (m, P - CH_2 - CH_3 , 9H). ^{19}F NMR (CDCl_3 , δ): at 15 °C, -113.5 (dm, 1 *o*-F); -114.5 (dm, 1 *o*-F); -115.6 (dm, 1 *o*-F); -116.9 (dm, 1 *o*-F); -162.3 (t, 1 *p*-F); -163.5 (t, 1 *p*-F); -164.3 (m, 1 *m*-F); -164.6 (m, 1 *m*-F); -164.8 (m, 1 *m*-F); -165.5 (m, 1 *m*-F). ^{31}P NMR (CDCl_3 , δ): at 15 °C, -8.7 (s). The complex is not sufficiently soluble for ^{13}C NMR.

Data for **12c'**. Anal. Calcd for $\text{C}_{33}\text{H}_{39}\text{F}_{10}\text{IrPPdSi}$: C, 35.70; H, 3.54. Found: C, 36.04; H, 2.98. MS: $m/z = 1015$ [$\text{M} - \text{C}_2\text{SiMe}_3 + 2\text{H}^+$] 8%; 573 [$\text{Cp}^*\text{IrI}(\text{PET}_3)^+$] 100%; 543 [$\text{Cp}^*\text{Ir}(\text{C}_2$

$\text{SiMe}_3)(\text{PET}_3)^+$] 43%; 455 [$\text{Cp}^*\text{IrI} + \text{H}^+$] 30%; 445 [$\text{Cp}^*\text{Ir}(\text{PET}_3)^+$] 21%. ^1H NMR (CDCl_3 , δ): at 15 °C, 2.14 (m, PCH_2CH_3 , 6H); 2.02 (s, Cp^* , 15 H); 1.09 (m, PCH_2CH_3 , 9H), -0.20 (s, SiMe_3 , 9H). ^{19}F NMR (CDCl_3 , δ): at 15 °C, -112.5 (dm, 1 *o*-F); -113.4 (dm, 1 *o*-F); -113.9 (dm, 1 *o*-F); -116.8 (dm, 1 *o*-F); -162.5 (t, 1 *p*-F); -162.6 (t, 1 *p*-F); -164.7 (m, 3 *m*-F); -165.3 (m, 1 *m*-F). ^{31}P NMR (CDCl_3 , δ): at 15 °C, -10.6 (s). Similar NMR patterns were observed at -50 °C. Due to the low solubility the ^{13}C NMR spectrum could not be registered.

X-ray Crystal Structure Determination of Complexes 5c, 7a, 7c, 8a-0.5CHCl₃, 9b, and 12a. Suitable crystals were obtained at low temperature (-30 °C) by cooling a concentrated solution of the complex in acetone/ethanol (1/2) (**5c**) or in acetone (**7a**) or by slow diffusion of Et_2O over chloroform (**7c**, **8a**) or dichloromethane (**9b**, **12a**) solutions of the complexes.

Crystal data and other details of the structure analyses are presented in Table 2. Crystals were fixed on top of quartz fibers and mounted on the diffractometers. Data were collected by $\omega/2\theta$ scans (**5c**, **7c**, **12a**), ω/θ scans (**7a**, **8a**), or ω scans (**9b**). Three check reflections remeasured at regular intervals showed no decay of the crystals over the period of data collection. The structures were solved by Patterson and Fourier methods. All non-hydrogen atoms were assigned anisotropic displacement parameters (except for Cp^* in **7a** and for the disordered solvent and C(11'), of a disordered phenyl group, in **8a**) and refined without positional constraints (except for the phenyl group (C(9)-C(14) and C(9')-C(14')) and solvent for **8a**). In complex **8a** the phenyl ring was refined as a rigid group. The disorder of this group arises because it is inclined but not perpendicular to the crystallographic mirror plane. Also, the anisotropically refined C(4) and F(3) have high displacement parameters, and disorder was observed in the phenyl group of the alkynyl ligands. A model in which two orientations of the aryl group were given equal weight allowed proper refinement of the structure. Solution in *Pna*2₁ for **8a** could not be carried out successfully. The hydrogen atoms in all complexes were constrained to idealized geometries and assigned isotropic displacement parameters 1.2 times the U_{iso} value of their attached atom, 1.5 times for the hydrogen methyl atoms. Final difference electron density map showed some peaks above 1 e Å⁻³ in the case of **5c**, **7a**, **8a**, and **12a**. They are probably due to a deficient absorption correction which may happen in the presence of heavy atoms. All calculations were carried out using the programs SHELXL-93⁴⁰ and SHELXTL-PLUS.⁴¹

Acknowledgment. We wish to thank the Comisión Interministerial de Ciencia y Tecnología (Spain, Project PB 95-0003-CO2-01,02) and the Universidad de La Rioja (Project API-98/B16) for their financial support.

Supporting Information Available: Tables giving positional and thermal parameters, bond distances, and bond angles for **5c**, **7a,c**, **8a**, **9b**, and **12a** (41 pages). Ordering information is given on any current masthead page.

OM980344M

(40) Sheldrick, G. M. SHELXL-93, a Program for Crystal Structure Determination; University of Göttingen, Göttingen, Germany, 1993.

(41) SHELXTL-PLUS, Software Package for the Determination of Crystal Structures, Release 4.0; Siemens Analytical X-ray Instruments Inc., Madison, WI, 1990.